3

Silencing of the microtubule-associated proteins doublecortin-like and doublecortin-like kinase-long induces apoptosis in neuroblastoma cells

Carla S Verissimo, Jan J Molenaar, John Meerman, Jordi Carreras Puigvert, Fieke Lamers, Jan Koster, Erik H J Danen, Bob van de Water, Rogier Versteeg, Carlos P Fitzsimons and Erno Vreugdenhil

Endocrine-Related Cancer (2010) 17: 399–414

ABSTRACT

Doublecortin-like kinase-long (DCLK-long) and doublecortin-like (DCL) are two splice variants of DCLK gene. DCL and DCLK-long are microtubule-associated proteins with specific expression in proliferative neural progenitor cells. We have tested the hypothesis that knockdown of DCL/DCLK-long by RNA interference technology will induce cell death in neuroblastoma (NB) cells. First, we analyzed the expression of DCL and DCLK-long in several human neuroblastic tumors, other tumors, and normal tissues, revealing high expression of both DCL and DCLK-long in NB and glioma. Secondly, gene expression profiling revealed numerous differentially expressed genes indicating apoptosis induction after DCL/DCLK-long knockdown in NB cells. Finally, apoptosis was confirmed by time-lapse imaging of phosphatidylserine translocation, caspase-3 activation, live/dead double staining assays, and fluorescence-activated cell sorting. Together, our results suggest that silencing DCL/DCLK-long induces apoptosis in NB cells.

INTRODUCTION

Neuroblastoma (NB) is a pediatric tumor arising from immature sympathetic neuroblast cells (Maris and Matthay, 1999). It is the most common solid cancer in childhood and the second highest cause of cancer deaths in children (Maris et al., 2007). NB exhibits characteristics of immature sympathetic neuroblasts (Brodeur, 2003). NBs contain a mixture of neuroblastic and neuroendocrine cell types that are organized in lobular structures with a central necrotic zone (Jogi et al., 2002; Poomthavorn et al., 2009). This pediatric tumor presents a broad spectrum of clinical behaviors. A subset of tumors undergoes spontaneous regression, while others show relentless progression (Castel et al., 2007; Maris et al., 2007; Tang et al., 2006). About half of all cases are classified as high-risk, with overall survival rates below 40%, despite intensive multimodal therapy (Maris et al., 2007). Microtubule-destabilizing agents, such as Vinca alkaloids, are used in NB treatment. However, NB patients develop pharmacoresistance to these chemotherapeutic agents, and systemic toxicity also occurs, which make NB difficult to treat (Don et al., 2004).

Studies have shown that microtubule-destabilizing agents block mitosis primarily by inhibiting the dynamics of spindle microtubules, leading to mitotic arrest (Jordan et al., 1992; Lobert et al., 1999). This arrest induces mitochondrial permeability transition, release of pro-death molecules into the cytosol, and caspase-dependent apoptosis of neoplastic cells (Bhalla, 2003). Different mechanisms have been highlighted linking mitotic arrest to the initiating events of the mitochondrial apoptosis pathway. These initiating events include either the direct inactivation of the anti-apoptotic Bcl2 by phosphorylation, or the activation of the pro-apoptotic molecules Bax and Bad, which in turn inactivate Bcl2 or Bcl-xL (Bhalla, 2003; Konishi et al., 2002; Yamaguchi and Wang, 2002).

Since NBs derive from proliferating neuroblasts, the study of genes involved in mitotic spindle formation in neuroblast is of specific interest to find new intervention points for NB treatment. We and others have recently identified and characterized one of such genes, doublecortin-like kinase (*DCLK1*). DCLK is a member of the doublecortin (DCX) gene family (Coquelle et al., 2006; Reiner et al., 2006) and regulates neurogenesis (Shu et al., 2006; Vreugdenhil et al., 2007), neuronal migration (Koizumi et al., 2006), retrograde transport of glucocorticoid receptors (GR; (Fitzsimons et al., 2008)), and mitotic spindle formation in neuroblasts (Shu et al., 2006; Vreugdenhil et al., 2007). The genomic organization of the *DCLK1* gene is rather complex and gives rise to numerous splice variants. The main splice variants encoded by *DCLK1* gene are doublecortin-like (DCL), DCLK-long, DCLK-short, and calcium/calmodulin-dependent protein kinase (CaMK)-related peptide (CARP; for the functional domains of these splice variants see Supplementary Figure S1). DCLK-long and DCL contain two DCX domains (Burgess and Reiner, 2000; Gleeson et al., 1999; Vreugdenhil et al., 2007), whereas DCLK-long and DCLK-short contain an additional CaMK-like domain (Schenk et al., 2007). CARP lacks both DCX and CaMK-like domains (Vreugdenhil et al., 1999). The microtubule-associated proteins (MAPs), DCL and DCLK-long, exhibit high homology with DCX (Shu et al., 2006; Vreugdenhil et al., 2007). DCX is a MAP involved in the regulation of microtubule dynamics, neuronal migration, and positioning in the neocortex (Bai et al., 2003). During embryonic development, both

DCL and DCLK-long are expressed specifically in areas of high neuroblast proliferation but not in other proliferative tissues (Vreugdenhil et al., 2007). Silencing of DCL/DCLK-long by RNA interference leads to disruption of the mitotic spindles and arrests the cells at prometaphase (Shu et al., 2006; Vreugdenhil et al., 2007). Interestingly, DCLK-long, DCLK-short, and CARP have been linked to apoptosis (Burgess and Reiner, 2001; Kruidering et al., 2001; Schenk et al., 2007).

Here, we study the expression and the consequences of DCL/DCLK-long knockdown in NB cells. We show for the first time that there is a specific expression of DCL and DCLK-long in human NBs and profound apoptosis induction after their knockdown, suggesting that these *DCLK1* gene splice products, which are specifically expressed in proliferative neuroblasts, are possible future therapeutic targets for the treatment of NB.

MATERIAL AND METHODS

Cell culture and transfection

Mouse N1E-115 and human SH-SY5Y NB cells were cultured as described (Molenaar et al., 2008; Vreugdenhil et al., 2007). Cells were grown in 24-well plates (Corning Life Sciences BV, Amsterdam, The Netherlands) coated with 100 ng/ml poly-L-lysine (Sigma–Aldrich, Inc). SH-SY5Y cells were seeded in plates coated with 100 mg/ml poly-D-lysine. For microscopy, both cell lines were grown in 24-well plates with glass bottom (Greiner Bio-One BV, Alphen aan den Rijn, The Netherlands) coated with 200 ng/ml poly-L-lysine (200 mg/ml poly-D-lysine for SH-SY5Y cells) at 80% confluence. The transfection of N1E-115 cells and the siRNAs (siDCL-1, siDCL-2, and siDCL-3) used were described by Vreugdenhil et al. 2007. SH-SY5Y cells were transfected with 200 nM siDCLK-4 (GCCCACUGCAGCUUCUACCTT-sense and GGUAGAAGCUGCAGUGGGCTT-antisense) and 200 nM siDCLK-5 (UGGAGUACACCAAGAAUGTT-sense and CAUUCUUGGUGUACUCCATT-antisense) siRNAs using lipofectamine 2000 (Invitrogen) as described in the manufacturer's protocol. AllStars Negative Control siRNA from Qiagen was used as negative control (NC). A transfection efficiency of 95 ± 5% was obtained, which was determined by quantifying the percentage of transfected cells with a non-targeting siRNA conjugated to FITC (Qiagen).

Protein extraction and western blots

Protein extraction, SDS-PAGE, and western blotting were performed as previously (Vreugdenhil et al., 2007). A previously described anti-CAMKLK1 antibody was used to detect DCL (Boekhoorn et al., 2008; Kruidering et al., 2001; Tuy et al., 2008; Vreugdenhil et al., 2007). CPG16 CaM Kinase VI antibody (Becton Dickinson BV, Breda, The Netherlands) was used for detecting DCLK-long. Relative optical densities were analyzed and quantified using ImageJ software (http://rsbweb.nih.gov/ij/; (Abramoff et al., 2004)) on images obtained from three independent blots. Alkaline phosphatase assay was performed using 30 U of alkaline phosphatase for 30 min at 30 ºC, followed by the addition of 10 mM sodium pyrophosphate as inhibitor (Francis et al., 1999).

Development of doxycycline-inducible stable cell line

N1E-115 cells ($1x10^6$) were transfected with 5 mg of a short hairpin RNA (shRNA) expression vector for DCL (TaconicArtemis, Cologne, Germany; (Seibler et al., 2007)) by cell electroporation using Amaxa Nucleofactor system (amaxa GmbH, Cologne, Germany) as described in the manufacturer's protocol. The medium was changed daily and replaced by medium containing 500 mg/ml G418 (Geneticin; Invitrogen). Two weeks after transfection, single clones were picked by standard procedures. The inducible DCL knockdown was tested by western blotting in samples from cells treated with 1 mg/ml doxycycline (Dox) for 3 days, refreshing the medium daily.

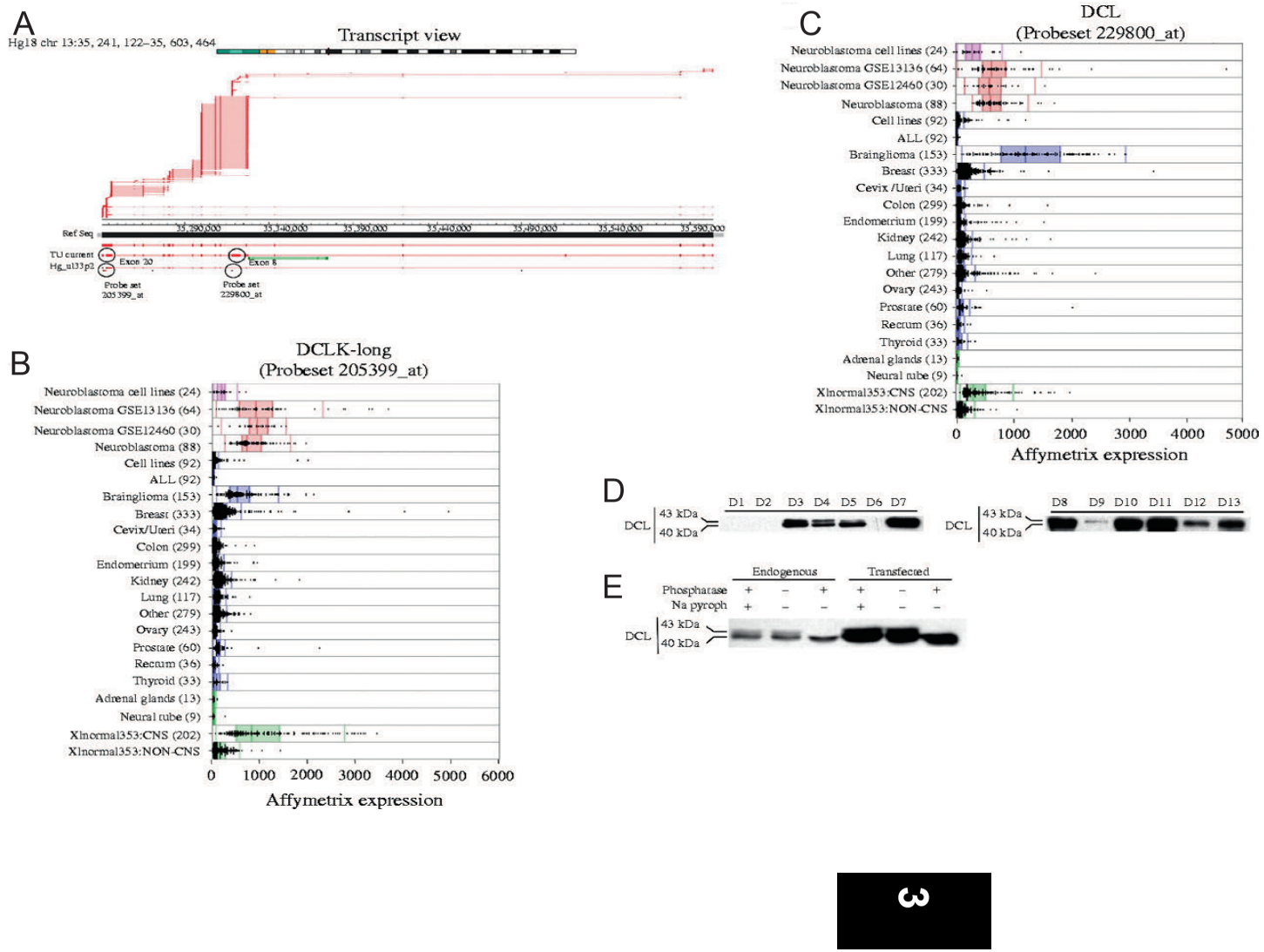
A
Hg18 chr 13:35, 241, 122–35, 603, 464
Transcript view
Ref Seq
TU current
Hg_u133p2
Exon 20
Exon 8
Probe set
205399_at
Probe set
229800_at
B
DCLK-long
(Probeset 205399_at)
Neuroblastoma cell lines (24)
Neuroblastoma GSE13136 (64)
Neuroblastoma GSE12460 (30)
Neuroblastoma (88)
Cell lines (92)
ALL (92)
Brainglioma (153)
Breast (333)
Cevix/Uteri (34)
Colon (299)
Endometrium (199)
Kidney (242)
Lung (117)
Other (279)
Ovary (243)
Prostate (60)
Rectum (36)
Thyroid (33)
Adrenal glands (13)
Neural tube (9)
Xlnormal353:CNS (202)
Xlnormal353:NON-CNS
0 1000 2000 3000 4000 5000 6000
Affymetrix expression
C
DCL
(Probeset 229800_at)
Neuroblastoma cell lines (24)
Neuroblastoma GSE13136 (64)
Neuroblastoma GSE12460 (30)
Neuroblastoma (88)
Cell lines (92)
ALL (92)
Brainglioma (153)
Breast (333)
Cevix /Uteri (34)
Colon (299)
Endometrium (199)
Kidney (242)
Lung (117)
Other (279)
Ovary (243)
Prostate (60)
Rectum (36)
Thyroid (33)
Adrenal glands (13)
Neural tube (9)
Xlnormal353:CNS (202)
Xlnormal353:NON-CNS
0 1000 2000 3000 4000 5000
Affymetrix expression
D
DCL
43 kDa
40 kDa
D1 D2 D3 D4 D5 D6 D7
D8 D9 D10 D11 D12 D13
E
Endogenous
Transfected
Phosphatase + – + + – +
Na pyroph + – – + – –
DCL
43 kDa
40 kDa

Figure 1 - Expression analysis of two splice variants of *DCLK1* gene in neuroblastomas and other tissues. (A) Analysis of the Affymetrix probesets using transcript view shows the known expressed sequence tags (ESTs) of the *DCLK1* gene locus. The probes target exon 8 (probeset 229800_at) and exon 20 (probeset 205399_at). RefSeq: reference sequence; TU Current: currently known Transcriptional Units, Hg_u133p2: probesets. The source for the public available data is given in the Materials and methods section. (B and C) Average microarray mRNA expression levels of DCLK-long (B) and DCL (C) splice variants in various adult tumor types (blue) and normal tissues samples (green) compared three independent neuroblastoma tumor series (red/pink). The number in brackets for each tissue type indicates the number of samples. (D) Western blotting of DCL expression at variable levels in neuroblastoma cell lines (D3, D4, D5, and D7), in other cell lines (D1 and D2), and in human primary neuroblastomas (D8–D13). D1, COS-1 cells; D2, Hela cells; D3, NG108-15 cells; D4, NS20Y cells; D5, N1E-115 cells; D6, marker; D7, SH-SY5Y cells. (E) Confirmation of differential DCL phosphorylation isoforms in NG108-15 cells. The higher molecular weight band visible in endogenous and transfected DCL corresponds to a phosphorylated form of DCL as shown by an alkaline phosphatase assay. This band is not observed in the presence of sodium pyrophosphate (Na pyroph), a phosphatase inhibitor, added prior to the phosphatase.

RNA isolation

RNA isolation, the concentration measurement, and the integrity determination were performed as described by Dijkmans et al., 2008.

Gene expression profiling from human samples and cell lines

The NB tumor panel used for Affymetrix HG-U133 Plus 2.0 Microarray analysis contains 88 NB samples derived from primary tumors of untreated patients. mRNA isolation and profiling methods were described previously (Molenaar et al., 2008). The expression data were normalized with the MAS5.0 algorithm within the Affymetrix's GCOS program. Target intensity was set to 100 (α1=0.04 and α 2=0.06). The mRNA profiles of two other NB panels, adult tumors, and normal tissues are publicly available and taken from the National Cancer Institute (NCI) Gene Expression Omnibus (GEO) database (GSE2109 (https://expo.intgen.org/geo/listPublicGeoTransactions.do) GSE4290 (http://rembrandt-db.nci.nih.gov), GSE2658 (http://lambertlab.uams.edu)). All data were analyzed using the R2 bioinformatic tool (http://r2.amc.nl, J Koster, personal communication). To identify correlating genes with the two DCLK splice variants in the 88-NB panel, the r value is calculated for all genes in the human genome (log2-transformed data are used). The significance of finding a certain correlation (P value) was calculated by the following formula: $t = \mathrm{r}/\sqrt{((1-\mathrm{r}^2)/(\mathrm{n}-2))}$, where r corresponds to the correlation value and n denotes the number of samples. Significance of gene enrichment in gene ontology (GO) categories was scored using 2×2 contingency table analysis (χ^2) with continuity correction.

Gene expression profiling from mouse NB N1E-115 cells

Sample preparation, hybridization to microarray, and detection were performed as described (Dijkmans et al., 2008). Raw signals were converted to expression values by Expression Array System Analyzer Software Version 1.1.1 (Applied Biosystems, Nieuwerkerk ad Ijssel, The Netherlands). Out of all 33 012 genes on the array, 14 076 (43%) had signal-to-noise ratio higher than 3, and were regarded as expressed in the N1E-115 cells. Subsequently, a quantile-normalization step was performed, and probe-to-gene annotation release version 12_05 was used for gene annotation. BRB-array software tools (Simon and Lam, 2006) were used to identify genes that were differentially expressed among classes using a random-variance t-test (Wright and Simon, 2003). Genes were considered statistically significant if their *P* value was < 0.001 and their false discovery rate was lower than 0.015, according to (Benjamini and Hochberg, 1995). We performed biological pathway analysis for the genes with *P* < 0.001. Differentially expressed GO groups of genes were identified as

follows. For each GO group, the number n of genes represented on the microarray in that group was calculated, and subsequently, the Fisher (LS) statistic and Kolmogorov–Smirnov (KS) statistic were performed as described (Simon and Lam, 2006). A GO category is regarded significantly differentially regulated if either significance level was < 0.01. All GO categories with between 5 and 100 genes represented on the array were considered. Differentially expressed Biocarta pathways were identified using the Hotelling T-square test.

Quantitative real-time PCR
Quantitative real-time PCR (RT-qPCR) was carried out by TaqMan technology using a Universal Probe Library (Roche) following the manufacturer's protocol.

Live/dead double staining and caspase-3 activation assays
Forty-eight hours after N1E-115 and SH-SY5Y NB cell transfection with siRNAs or induction for 3 days with Dox, live/dead double staining assay (Calbiochem, San Diego, CA, USA) was performed as described in the manufacturer's protocol. To detect caspase-3 activation, N1E-115 cells were imaged in the presence of 'Nuncview' Alexa-488-labeled caspase-3 substrate (Biotium Inc., Hayward, CA, USA) as indicated in the manufacturer's protocol. N1E-115 cells treated with 20 nM staurosporine (STS; Sigma–Aldrich, Inc.) for 3 h were used as positive control. STS is a kinase inhibitor known to induce apoptosis (Lopez and Ferrer, 2000). SH-SY5Y human NB cells incubated for 5 h with 500 nM STS were used as positive control. Differential interference contrast (DIC) and fluorescence imaging were performed on a Nikon TE-2000 E system under 37 ºC and 5% CO2 controlled conditions.

Time-lapse imaging of phosphatidylserine translocation
Forty-eight hours after N1E-115 cells had been transfected, time-lapse imaging of phosphatidylserine (PS) translocation was performed as described recently (Puigvert et al., 2010; Puigvert et al., 2009) for a period of 19 h. Cells treated with 20 nM STS (Sigma–Aldrich, Inc.) for 3 h were used as positive control. DIC and fluorescence imaging were performed on a Nikon TE-2000 E system under 37 ºC and 5% CO2 controlled conditions.

Image analysis and cell counting
ImageJ software (Abramoff et al., 2004) was used for image analysis and cell counting. Time-lapse images were processed with Image-Pro Plus (Version 5.1; Media Cybernetics).

Fluorescence-activated cell sorting
Fluorescence-activated cell sorting (FACS) analysis was performed as described previously with some changes (Puigvert et al., 2009). Forty-eight hours after transfection, cells seeded in 24-well plates were trypsinized, washed with PBS, resuspended in PBS/EDTA (4 mM), and fixed in 67% ethanol overnight at -20 ºC. Cells were stained with FACS staining solution (1 mg/ml propidium iodide, 10 mg/ml RNase A, and PBS) for 45 min in the absence of light at room temperature. After resuspension, 5000–10 000 cells were analyzed by flow cytometry on a FACSCalibur (Becton Dickinson). The CellQuest software (Becton Dickinson) was used for data analysis.

Statistical analysis
Unless otherwise indicated, assays were carried out for three independent experiments run in triplicates. Results are expressed as mean ± S.E.M. Where appropriate, Student's t-test was done, and $P < 0.05$ was considered statistically significant.

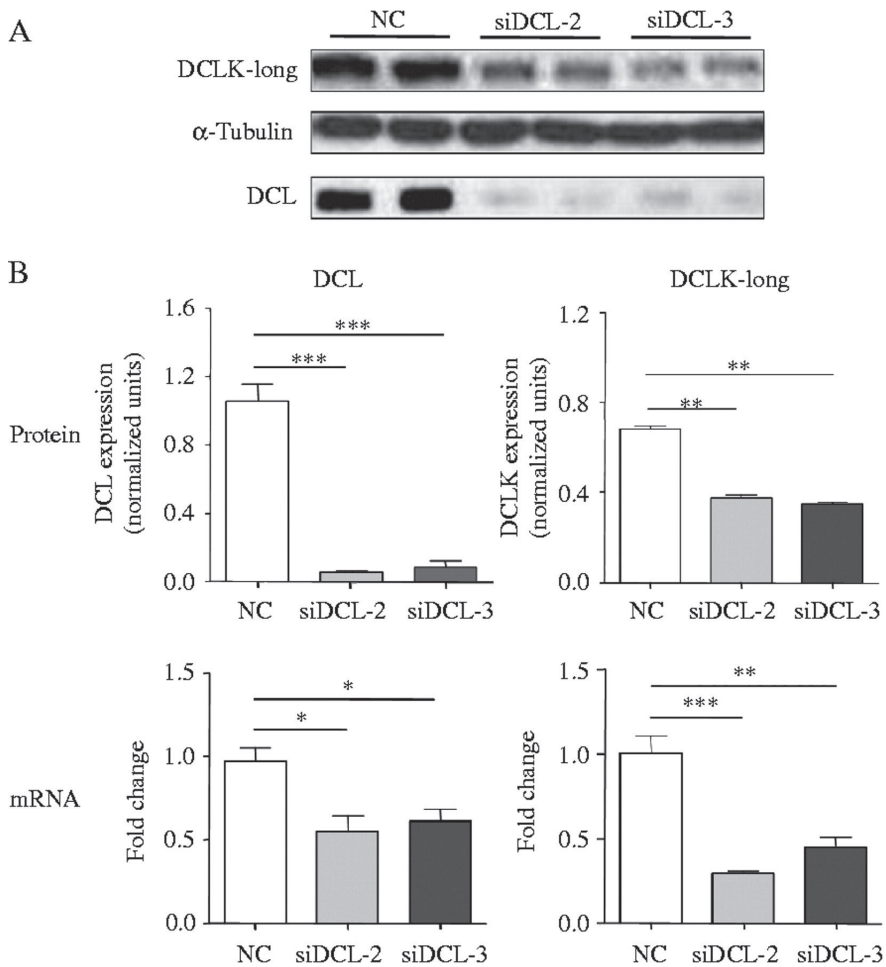

Figure 2 - DCLK-long and DCL silencing in transfected N1E-115 mouse neuroblastoma cells at 48 h after transfection with synthetic siRNAs siDCL-2, siDCL-3, and negative control siRNA. (A) Western blotting results of DCL and DCLK-long expression. (B) Expression of DCL and DCLK-long at protein and mRNA levels. NC, negative control. The protein expression was normalized to α-tubulin, and the mRNA was normalized to GAPDH. Columns, mean of three independent experiments (n=6); bars, S.E.M. *, $P < 0.05$. **, $P < 0.01$. ***, $P < 0.001$.

RESULTS

DCL and DCLK-long mRNAs are highly expressed in human NBs

To evaluate mRNA expression levels of DCL and DCLK-long in our previously described neuroblastic tumor panel (Molenaar et al., 2008), we used the bioinformatic platform R2 identifying their expression levels in different tumors, in normal tissues, and in cell lines (http://r2.amc.nl, J Koster, personal communication). It also allowed us to predict their involvement in specific signal

transduction routes. This application uses a database that contains 19 438 microarrays of 20 845 tumors and normal tissue samples. First, we analyzed the expression of DCLK in neuroblastic tumors (Fig. 1). The R2 platform is linked to the TranscriptView web application (Valentijn et al., 2006), which we used to identify the position of the probesets on transcription variants (Fig. 1A). There are two Affymetrix 133U plus2 microarray probesets annotated to the *DCLK1* gene locus. Probeset 205399_at targets exon 20 of the *DCLK1* gene, which is only transcribed in DCLK-long and DCLK-short variants ((Vreugdenhil et al., 2001); Fig. 1A). Probeset 229800_at targets exon 8, which is transcribed in DCL and CaMK-CARP transcripts ((Vreugdenhil et al., 2007); Fig. 1A). DCLK-short and CARP have been detected in adult neuronal cells but not in neuroblasts (Burgess and Reiner, 2002; Engels et al., 2004; Vreugdenhil et al., 2001). Since exon 8 and exon 20 are mutually exclusive, we can use the corresponding probesets to separately analyze the expression of DCL and DCLK-long transcriptional variants. We compared the expression of both transcripts in the NB datasets with expression in various other tumors and normal tissues. The bar plot of Fig. 1B shows an increased DCLK-long expression in NB compared with various adult tumor types and normal non-nervous tissues. Expression in NBs was in the same range as the expression in adult central nervous system (CNS), as expected, since the probeset also recognizes other DCLK splice variants (Fig. 1A), highly expressed in different areas of the adult brain (Burgess and Reiner, 2002; Engels et al., 2004; Vreugdenhil et al., 2001). With the exon 8 probeset, we identified abundant DCL expression in NB compared with other tissue types. Interestingly, only gliomas showed comparable expression levels (Fig. 1C). To analyze a putative correlation between the two probesets, we used gene expression profiles from 88 NBs (see Materials and methods for statistical tests). No significant correlation was found between DCL and DCLK-long expression, as measured with exon 8 or exon 20 probesets, suggesting that both splice variants may have different expression profiles as expected from their embryonic expression (Boekhoorn et al., 2008; Lin et al., 2000; Vreugdenhil et al., 2007).

To estimate the signal transduction pathways in which DCLK variants are involved, we searched for genes with correlating expression patterns. This analysis revealed 1206 genes with a significant correlation ($P < 0.01$) with DCLK-long. This gene set exhibits enrichment of genes involved in microtubule-based processes and axon projection (see Supplementary Table S1). The same analysis for DCL showed 880 genes with a significant correlation ($P < 0.01$). Interestingly, this correlation was most significant for GO clusters involved in mitochondrial respiratory chain processes (see Supplementary Table S2), suggesting a link between DCL and mitochondria. In silico analysis, using PSORT II software (http://psort.ims.u-tokyo.ac.jp/; (Nakai and Horton, 1999)), of the subcellular localization of human DCL also predicts that 17.4% of this MAP is located in mitochondria (see Supplementary Table S3).

DCL and DCLK-long proteins are expressed in human NBs and in NB cell lines

The above-mentioned experiments provided important information on the expression of DCL and DCLK-long mRNA in NBs. Western blotting showed expression of the DCL protein in different human NBs (Fig. 1D), validating the

observation done at the mRNA level. Moreover, DCL and DCLK-long proteins were also detected in mouse and human NB cell lines (Figs 1D and 2), and were not observed in non-NB cell lines (Fig. 1D). In Fig. 1E, we demonstrate that the double band detected in the NG108-15 cell line represents differentially phosphorylated DCL isoforms, as described previously by other authors (Friocourt et al., 2003; Tuy et al., 2008). The molecular weight values estimated for the two DCL bands are in high correlation with those previously described in the literature.

Synthetic modified siRNAs silence DCL/DCLK-long in mouse NB cells

To study the consequences of DCL/DCLK-long knockdown, a mouse N1E-115 NB cell line that endogenously expresses these MAPs was used. Three previously described and validated synthetic siRNAs were utilized (Vreugdenhil et al., 2007); two of them, siDCL-2 and siDCL-3, effectively knocked down DCL, while the third one, siDCL-1, was not effective. In parallel, a synthetic non-targeting siRNA (AllStars Negative Control siRNA, Qiagen) was used as an independent NC. Since no significant differences were found between the two NC siRNAs (see Supplementary Figure S2), we present only the results obtained with the NC siDCL-1 (indicated as NC in the figures). Both siDCL-2 and siDCL-3 silenced DCL more effectively than they silenced DCLK-long at the protein level (Fig. 2). Nevertheless, the knockdown detected by RT-qPCR was ~50% for both MAPs (Fig. 2B), suggesting the existence of posttranslational regulatory mechanisms.

Apoptotic pathways are affected after DCL/DCLK-long knockdown

To investigate the effect of the knockdown of DCL/DCLK-long at the molecular level, we have used gene expression profiling of N1E-115 cells. Hierarchical gene cluster analysis showed clustering of siDCL-3 and siDCL-2 samples versus samples of NC (Fig. 3A). Comparing siDCL-2 and NC, samples resulted in the identification of 1034 differentially expressed genes, while 931 differentially expressed genes were identified with siDCL-3. Of these differentially expressed genes, 663 genes were in common (Fig. 3B). The majority of these 663 genes were up-regulated (562) and 101 were down-regulated (Fig. 3B). Pathway analysis resulted in the identification of significant overrepresented pathways related to cell cycle, oxidative stress, and apoptosis (Table 1). Pax6 was one of the most up-regulated genes in our expression profiling studies. The up-regulation of Pax6 has been linked to the inactivation of neuroblast proliferation, apoptosis, and acquisition of neuronal cell fate (Berger et al., 2007). Moreover, Bax is an example of an apoptotic inducer (Nutt et al., 2002) found up-regulated in the affected pathways. Oxidative phosphorylation and ATP synthesis were among the most affected biological processes (see Supplementary Table S5). Genes such as Ndufa1 (Mamelak et al., 2005) and Cox7c (Lenka et al., 1998) were up-regulated (Fig. 3C and Supplementary Table S4), indicating an active oxidative phosphorylation process in cells with decreased DCL/DCLK-long expression. Moreover, mitochondria were among the most affected cellular components (see Supplementary Table S5). Differential expression of several selected genes was confirmed by RT-qPCR (see Supplementary Table S6). Together, these data suggest that DCL/DCLK-long knockdown leads to apoptosis.

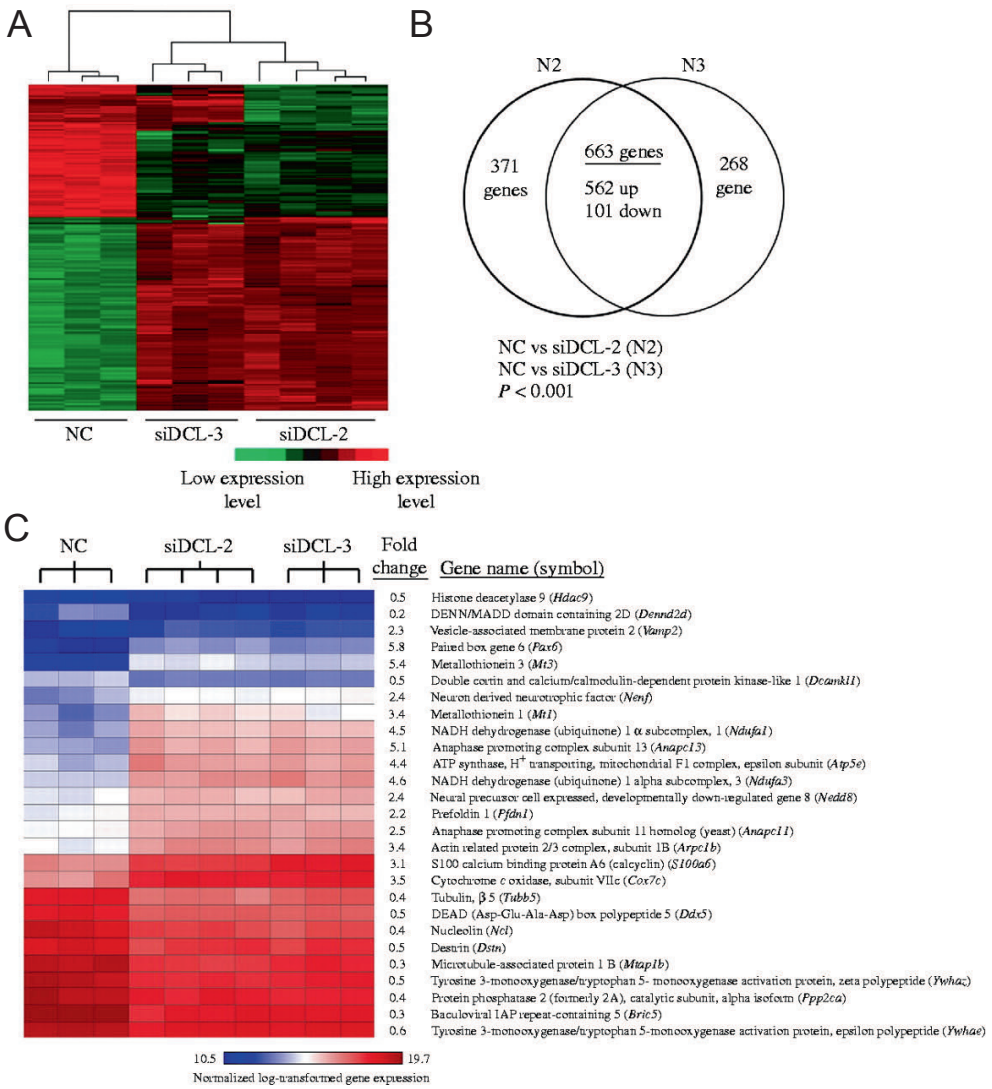

Figure 3 - mRNA expression profiling of N1E-115 mouse neuroblastoma cells at 48 h after transfection. Cells were transfected with siDCL-2, siDCL-3, and negative control (NC) siRNAs. (A) Hierarchic clustering of the mRNA expression profiling in the different groups; green indicates reduced expression and red indicates induced expression. (B) Venn diagram highlighting the overlap of differentially expressed genes between negative control and siDCL-2 groups (N2) and negative control and siDCL-3 groups (N3). The total number of up- and down-regulated genes is indicated. (C) Normalized log-transformed gene expressions for a selection of the overlapping 663 genes. Blue, low normalized log-transformed gene expression; red, high normalized log-transformed gene expression. Microarray analyses were performed using four biological replicates (nZ4) per condition. One biological replicate of the negative control group and one of siDCL-3 group were excluded from the analysis because they did not fulfill the microarray quality control criteria. The analysis was performed for a P value lower than 0.001 and a false discovery rate (FDR) lower than 0.015.

Silencing of DCL/DCLK-long leads to apoptosis in N1E-115 NB cells

Since the above-described microarray results suggest apoptosis induction by DCL/DCLK-long knockdown in NB cells, we performed biochemical assays to investigate this possibility.

Time-lapse imaging of PS translocation (Puigvert et al., 2010; Puigvert et al., 2009) showed a significant difference between the NC and cells transfected with the effective siRNAs at the different time points (Fig. 4A and B and Supplementary Video 1). After counting the number of cells presenting FITC-labeled Annexin-V conjugated to PS at different time points, we identified an increase of PS translocation to the outer membrane in cells with DCL/DCLK-long knockdown (Fig. 4A and B), showing an increase of apoptosis in these cells. At the beginning of the assay (48 h after transfection), 10.33 ± 1.20% apoptotic cells were quantified for siDCL-2, and 16.71 ± 5.07% apoptotic cells were quantified for siDCL-3, while 6.93 ± 0.90% apoptotic cells were detected in the NC (Fig. 4B). Eighteen hours after starting the assay (66 h after transfection), 79.92 ± 0.93% cells transfected with siDCL-2 and 89.18 ± 5.32% cells transfected with siDCL-3 were positive for FITC-labeled Annexin-V conjugated to PS. These values were significantly higher ($P < 0.05$) than those in the NC (51.82 ± 3.08%; Fig. 4B). Our results indicate that DCL/DCLK-long knockdown leads to apoptosis.

We also performed double staining assays to discriminate between live and dead cells (Fig. 4C; (Balcer-Kubiczek et al., 2006)). In line with our PS translocation studies, DCL/DCLK-long knockdown leads to a significantly higher ($P < 0.05$) number of dead cells 48 h after transfection with the two effective siRNAs. 22.01 ± 1.62% N1E-115 cells transfected with siDCL-2 and 18.43 ± 1.31% N1E-115 cells transfected with siDCL-3 presented membrane damage, which was indicated by propidium iodide staining. Significantly less ($P < 0.05$; 9.36 ± 0.90%) NC cells were positive for propidium iodide (Fig. 4C). Using an Alexa-488-labeled caspase-3 substrate (Puigvert et al., 2010), caspase-3 activation was also measured. Compared with the NC (11.53 ± 1.53%), a significant increase in percentage of cells with active caspase-3 was detected when transfected with siDCL-2 (16.83 ± 1.37%; $P < 0.05$) and siDCL-3 (29.61 ± 2.41%; $P < 0.001$; Fig. 4D).

FACS corroborated the effects of DCL/DCLK-long silencing (Fig. 5). For FACS analysis, we used cells transduced with siDCL-3 due to its higher effectiveness in inducing cell death (Fig. 4). We observed a significantly higher ($P < 0.05$) percentage of apoptotic cells (18.45 ± 1.00%) in cells treated with siDCL-3 than in cells treated with the NC (10.39 ± 1.61%). At this time point, no significant differences were detected in cell-cycle progression among the different experimental groups.

To validate the specificity of the observed effects, an inducible stable cell line was developed to express specific shRNAs (Fig. 6). First, we attempted to develop a stable cell line with constitutive expression of shRNA against DCL. However, the cells failed to survive, in agreement with the observed effects of DCL knockdown on cell survival using synthetic siRNAs. Nevertheless, DCL knockdown was possible using a Dox-inducible expression of specific shRNAs against DCL. By western blotting, we detected DCL knockdown in cells treated with Dox (88.67 ± 2.68% in colony 1 and 63.84 ± 5.66% in colony 6), while cells treated with vehicle depicted DCL levels comparable to the parental cell line (Fig. 6A and B).

Table 1 - Examples of affected pathways in mouse N1E-115 neuroblastoma cells with doublecortin-like (DCL) and doublecortin-like kinase-long (DCLK-long) knockdown. Sixty-eight pathways (Biocarta pathways) were significant at the nominal 0.0005 level of the Hotelling T-square test.

Biocarta pathway	Hotelling's test *P* value	Modulated genes
Protein kinase A at the centrosome	2.00×10^{-7}	Ppp2r1a (↓↓); Prkar2a (↓↓); Cyp51 (↓↓); Rhoa (↓↓); Akap9 (↑↑); Prkar2b (↓↓); Prkaca (↑↓); Prkce (↓↓)
Regulation of Bad phosphorylation	7.40×10^{-6}	Ywhah (↓↓); Bax (↑↑); Mapk1 (↓↓); Igf1 (↓↑); Asah1 (↓↓); Bad (↑↑); Pik3r1 (↑↓); Mapk3 (↓↓); Akt1 (↓↓); Rps6ka1 (↓↓); Bcl2l1 (↓↓); Prkaca (↑↓); Bcl2 (↓↓)
AKAP95 role in mitosis and chromosome dynamics	1.26×10^{-5}	Ddx5 (↓↓); Ppp2r1a (↓↓); Prkar2a (↓↓); Akap8 (↓↓); Prkar2b (↓↓); Prkaca (↑↓)
Control of skeletal myogenesis by HDAC and calcium/calmodulin-dependent kinase (CaMK)	2.12×10^{-5}	Ywhah (↓↓); Igf1r (↓↑); Ppp3ca (↓↓); Pik3r1 (↑↓); Akt1 (↓↓); Hdac5 (↓↑); Mapk7 (↓↑); Camk2a (↑↑); Mapk14 (↓↓); Mef2a (↓↓); Calm1 (↓↑); Myod1 (↑NA)
Multiple antiapoptotic pathways from IGF1R signaling lead to Bad phosphorylation	2.43×10^{-5}	Ywhah (↓↓); Mapk1 (↓↓); Igf1r (↓↑); Raf1 (↓↓); Asah1 (↓↓); Pik3ca (↓↓); Grb2 (↓↓); Bad (↑↑); Irs1 (↓↓); Map2k1 (↓↓); Mapk3 (↓↓); Akt1 (↓↓); Rps6ka1 (↓↓); Ppp1r13b (↓↑); Sos1 (↑↑); Hras1 (↑↑); Prkaca (↑↓); Shc1 (↓↓)
Oxidative stress induced gene expression via Nrf2	2.65×10^{-5}	Hmox1 (↑↓); Sirt7 (↑↑); Mapk1 (↓↓); Jun (↑↑); Atf4 (↓↓); Nfe2l2 (↓↓); Mafg (↑↑); Creb1 (↓↓); Cryz (↓↓); Keap1 (↑↓); Fos (↑↑); Prkcb1 (↓↓); Por (↑↑); Mapk14 (↓↓); Maff (↑↑); Mafk (↓↓)
Cell cycle: G2/M checkpoint	3.10×10^{-5}	Ywhah (↓↓); Chek1 (↓↓); Cdc34 (↑↑); Myt1 (↓↓); Cdkn1a (↓↓); Wee1 (↓↓); Brca1 (↓↓); Gadd45a (↑↑); Mdm2 (↓↓); Rps6ka1 (↓↓); Atm (↑↑); Atr (↓↓); Cdc25c (↓↓); Trp53 (↓↓); Cdkn2d (↑↑); Plk1 (↓↓); Prkdc (↓↓); Ywhaq (↓↓)
Role of Ran in mitotic spindle regulation	3.83×10^{-5}	Kpna2 (↓↓); Aurka (↓↓); Kpnb1 (↓↓); Tpx2 (↓↓); Kif15 (↑↓); Rcc1 (↓↓); Ranbp1 (↓↓); Rangap1 (↓↓)
P53 signaling pathway	1.63×10^{-4}	Ccnd1 (↓↓); Bax (↑↑); Cdkn1a (↓↓); Gadd45a (↑↑); Mdm2 (↓↓); Cdk4 (↑↓); Ccne1 (↑↑); Atm (↑↑); Pcna (↓↓); E2f1 (↑↑); Trp53 (↓↓); Apaf1 (↓↓); Bcl2 (↓↓)
Regulation of MAP kinase pathways through dual specificity phosphatases	2.05×10^{-4}	Dusp2 (↓↓); Dusp6 (↓↓); Dusp1 (↓↓); Mapk3 (↓↓); Dusp9 (↓↓); Mapk14 (↓↓); Dusp8 (↑↑); Dusp4 (↑↑)
Apoptotic signaling in response to DNA damage	3.63×10^{-4}	Bax (↑↑); Bid (↓↓); Cycs (↑↑); Bad (↑↑); Akt1 (↓↓); Atm (↑↑); Casp3 (↑↑); Tln1 (↑↑); Bcl2l1 (↓↓); Prkcb1 (↓↓); Prp1 (↓↓); Casp9 (↓↑); Trp53 (↓↓); Casp7 (↓↓); Apaf1 (↓↓); Bcl2 (↓↓); Stat1 (↑↑)
Apoptotic DNA fragmentation and tissue homeostasis	4.64×10^{-4}	Hmgb1 (↓↓); Top2a (↓↓); Dffa (↓↓); Endog (↑↑); Hmgb2 (↑↑); Casp3 (↑↑); Casp7 (↓↓); Cad (↓↓)

(↑↑), up regulated in both comparisons (negative control vs. siDCL-2 and negative control vs. siDCL-3); (↓↓), down regulated in both comparisons; (↑↓), up regulated in the comparison negative control vs. siDCL-2 and down regulated in the comparison negative control vs. siDCL-3; (↓↑), down regulated in the comparison negative control vs. siDCL-2 and up regulated in the comparison negative control vs. siDCL-3; (↑NA), up regulated in the comparison negative control vs. siDCL-2 and not altered for the second comparison.

Using these stable cell lines, we observed that DCL knockdown induced a significant increase in cell death ($P < 0.05$; Fig. 6C and D). In Dox-treated cells, 23.44 ± 3.39% (colony 1) and 16.82 ± 3.13% (colony 6) of dead cells were detected. In contrast, 11.77 ± 0.13% (colony 1, no Dox), 7.00 ± 3.25% (colony 6, no Dox), 6.00 ± 3.14% (parental cell line with Dox), and 7.55 ± 0.22% (parental cell line no Dox) of dead cells were detected (Fig. 6C and D). These results showed that a higher percentage of cell death was observed in cells that presented a higher DCL knockdown (colony 1, Dox). Moreover, a similar percentage of knockdown obtained with siRNA, ~90% (Fig. 2), leads to a comparable percentage of cell death, around 20% (Fig. 4C).

DCL/DCLK-long knockdown in human SH-SY5Y NB cells leads to cell death

To confirm the results obtained in mouse N1E-115 NB cells, we knocked down DCL/DCLK-long in human NB cells. The expression of DCL and DCLK-long was checked in different human NB cell lines by gene expression profiling. To avoid a possible compensation of DCL/DCLK-long function by other members of the DCX family (Koizumi et al., 2006), SH-SY5Y cells were selected. This cell line presents high expression of DCL and DCLK-long and low expression of DCX (Fig. 7A). In addition, this cell line presents a high rate of cell division, allowing us to perform the studies in the same time frame as with mouse NB cells. Using two effective siRNAs, siDCLK-4 and siDCLK-5, we obtained a significant DCL/DCLK-long knockdown (Fig. 7B and Supplementary Figure S3). We got 71.04 ± 4.42% DCL knockdown with siDCLK-4 and 65.20 ± 0.79% DCL knockdown with siDCLK-5 (Fig. 7B). 72.56 ± 2.08% DCLK-long knockdown was quantified using siDCLK-4 and 52.84 ± 1.63% DCLK-long knockdown was quantified using siDCLK-5 (Fig. 7B). Using live/dead double staining as with mouse NB cells, we found 27.80 ± 1.38% dead cells using siDCLK-4 and 26.30 ± 2.88% dead cells using siDCLK-5 (Fig. 7C and D), which was significantly higher ($P < 0.01$ and $P < 0.001$ respectively) than the 10.64 ± 2.18% detected in cells treated with NC siRNA (Qiagen; Fig. 7C and D). Thus, silencing DCL/DCLK-long by synthetic siRNAs in human SH-SY5Y NB cells induced a significant increase in cell death.

DISCUSSION

In the present work, we demonstrate for the first time the expression of the two MAPs DCL and DCLK-long in human NBs, and using different experimental strategies ranging from gene expression profiling to live-imaging studies, we show that DCL and DCLK-long are crucial for the proliferation and survival of NB cells. Both DCL and DCLK-long, proteins derived from the *DCLK1* gene, are highly expressed in human NBs. Similarly, both are expressed in mouse N1E-115 and human SH-SY5Y NB cells. We demonstrated that silencing of these MAPs by RNA interference leads to apoptosis in mouse and human NB cells. Therefore, our data suggest that DCL and DCLK-long may be a potential therapeutic target for NB.

MAPs play a role in tumor cell resistance to microtubule-destabilizing agents by regulating microtubule dynamics (Bhat and Setaluri, 2007). Nevertheless, in some cases, NB patients are treated with combination chemotherapy. Therefore, the development of resistance to microtubule-destabilizing agents, such as Vinca alkaloids, cannot be studied in these patients. However, an increase in

microtubule-stabilizing proteins leads to resistance to Vinca alkaloids in NB cell lines (Don et al., 2004). This, in addition to the observation that DCL/DCLK-long silencing in NB cell lines leads to microtubule destabilization (Vreugdenhil et al., 2007), suggests that targeting microtubule-stabilizing proteins, such as DCL/DCLK-long, may reduce the development of chemoresistance to microtubule-destabilizing agents.

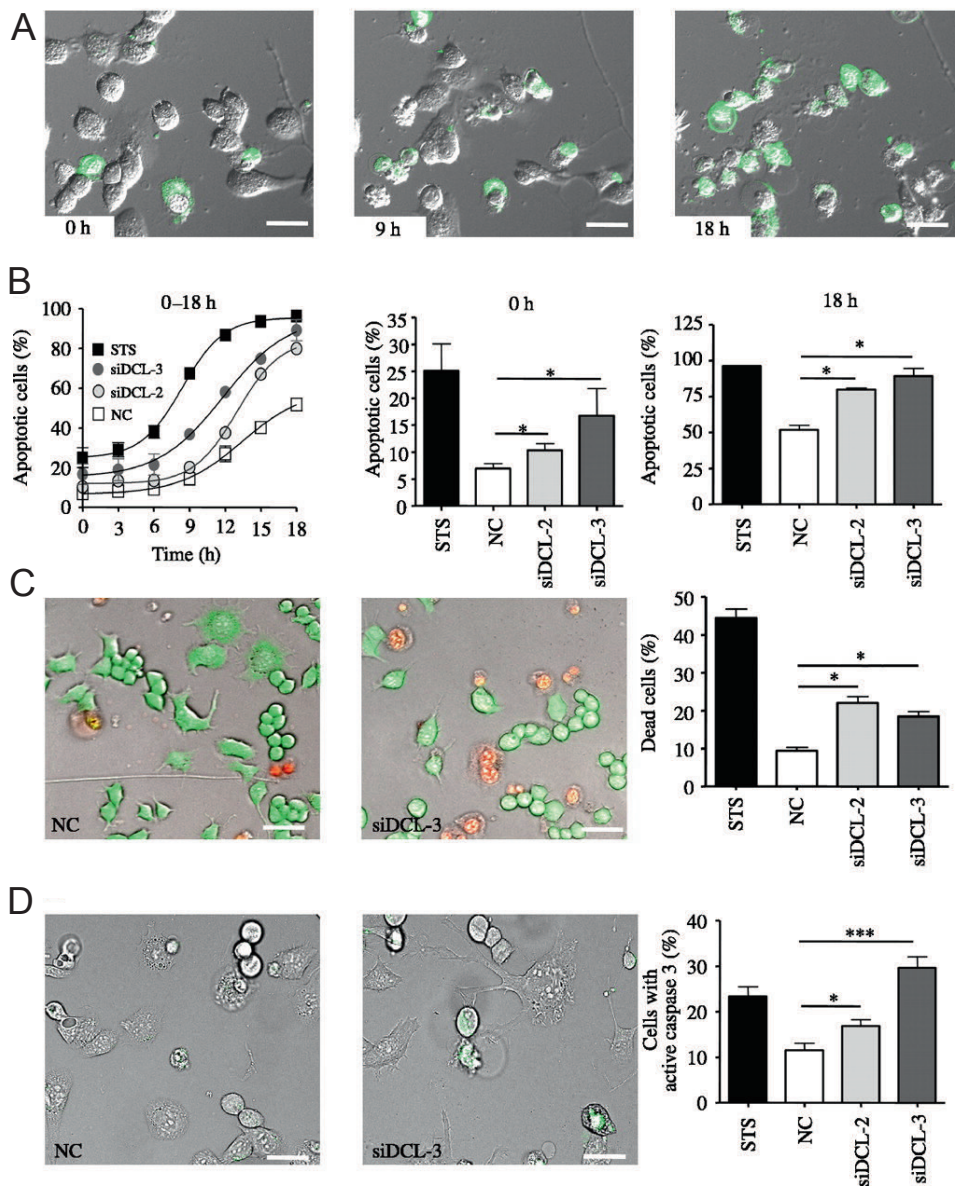

Figure 4 - Apoptosis studies in mouse N1E-115 neuroblastoma cells at 48 h after transfection. (A and B) Time-lapse imaging of phosphatidylserine translocation. Images were taken at 30 min interval (see

Supplementary Video 1). (A) Time-lapse imaging 0, 9 and 18 h after starting the assay. (B) Percentage of cells with translocated phosphatidylserine at different time points for the different treatments. The initial time point of the assay (0 h) corresponds to 48 h after transfection. (C) Live/dead double staining. Viable cells are stained with a cell-permeable green fluorescent cyto-dye and dead cells are stained with both cyto-dye (green) and propidium iodide (red). (D) Caspase-3 activation assay. Bar graph shows the percentage of cells with active caspase-3. STS, staurosporine. NC, negative control. Overlap of DIC and fluorescent imaging were used in the different assays. 20x magnification. Scale bars, 50 mm. Data points and Columns, mean of two independent experiments (n=6); bars, S.E.M. *, $P < 0.05$. ***, $P < 0.001$.

The mechanisms by which DCL and DCLK-long stabilize microtubules seem similar to that of the highly homologous DCX (Shu et al., 2006). DCL and DCLK-long as well as DCX have been shown to be crucial for neuronal proliferation, migration, and axonal outgrowth (Deuel et al., 2006; Koizumi et al., 2006; Shu et al., 2006; Vreugdenhil et al., 2007). In agreement with this, we detected a significant correlation between DCLK-long and genes involved in microtubule-based processes and axon projection human NB samples.

Our results show higher expression of DCL and DCLK-long in human NBs compared with various other tumor types and with normal non-nervous tissue. At the protein level, different DCL phosphorylated isoforms were detected in NB cell lines. Further research is needed to confirm the presence of phosphorylated DCL isoforms in NB tumors. Interestingly, DCL was also highly expressed in gliomas, in agreement with our previous findings showing high expression of this MAP in radial glial cells (Vreugdenhil et al., 2007). DCL expression in radial glial cells was shown to be crucial for proliferation and stability of the early radial glial scaffold (Vreugdenhil et al., 2007). Consistently, gliomas are a collection of tumors that occur within the CNS and arise from astrocytes, oligodendrocytes, or their precursors, radial glial cells (Anthony et al., 2004; Holland, 2001). Therefore, our results indicate that DCL might also be a target of interest for glioma therapy.

Using two different specific siRNAs, siDCL-2 and siDCL-3, targeting completely different regions of the mRNA, we silenced the expression of DCL/DCLK-long in mouse NB cells, which endogenously expressed these MAPs (Vreugdenhil et al., 2007). Gene expression profiling after knockdown revealed an extensive overlap of the gene expression using the two effective siRNAs. The genes identified in non-overlapping groups might be due to off-target effects or due to distinct potencies of the two siRNAs used in these studies. Using the two siRNAs, siDCL-2 and siDCL-3, we observed coherent phenotype. This strongly suggests that the observed effects may not be due to off-targets of the individual siRNAs. Moreover, cell death due to DCL knockdown was confirmed in a shRNA-inducible stable cell line. A similar percentage of DCL knockdown obtained with synthetic siRNA and Dox-inducible shRNA leads to a comparable percentage of cell death in N1E-115 cells. This also indicates that DCL has a more relevant role in cell survival than DCLK-long, therefore suggesting that the activation of the apoptotic process is related to the microtubule-binding domains of these MAPs and not to the kinase domain of DCLK-long.

Analysis of the genes that were modulated in common by using siDCL-2 and siDCL-3 strongly indicates a specific induction of apoptosis. Consistent with this conclusion, the activation of Pax6, one of the most up-regulated genes in our

expression profiling studies, leads to inactivation of neuroblast proliferation, apoptosis, and acquisition of neuronal cell fate (Berger et al., 2007). Oxidative stress pathways were also identified, supporting the idea that silencing DCL/DCLK-long leads the cells toward apoptosis. The induction of apoptosis by oxidative stress via mechanisms that involve mitochondria has been extensively documented (Green and Reed, 1998; Nazarewicz et al., 2007). Furthermore, oxidative phosphorylation was found among the most overrepresented biological processes and mitochondria were found to be one of the cell components most affected. Interestingly, down-regulation of genes involved in mitochondrial function and oxidative phosphorylation pathway has been shown to be a consistent feature of many tumors (Mamelak et al., 2005). One of those genes is NDUFA1, which was up-regulated in mouse NB cells by DCL/DCLK-long knockdown. Moreover, a relation between oxidative phosphorylation, mitochondria, and apoptosis has been suggested (Green and Reed, 1998). Disruption of electron transport in the oxidative phosphorylation process has been recognized as an early feature of cell death (Green and Reed, 1998).

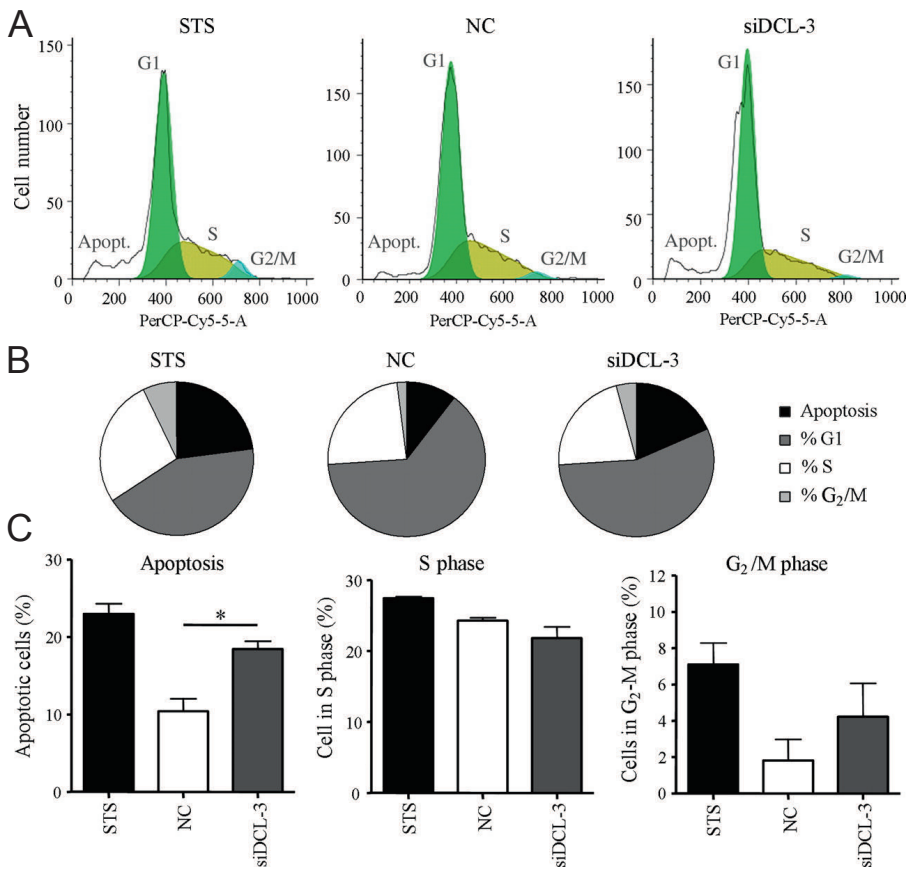

Figure 5 - Fluorescence-activated cell sorting results of neuroblastoma cells with DCL/DCLK-long knockdown. (A) Histogram representation of cell population 48 h after transfection with siDCL-3 or with the negative control siRNA (NC). Data shown are representative of four independent experiments. (B)

Pie graphs of the effect of DCL and DCLK-long knockdown on the distribution of mitotic cells in different phases and on the induction of apoptosis. (C) Bar graphs of cells in apoptosis, in S phase, and in G2-M phase. A significantly higher percentage of apoptotic cells were found in the siDCL-3 group than in the negative control. No significant difference was found between NC and cells with the knockdown (siDCL-3) in the S and G2-M phases of the cell cycling. STS, staurosporine. Columns, mean of four independent experiments (n=4); bars, S.E.M. *, $P < 0.05$.

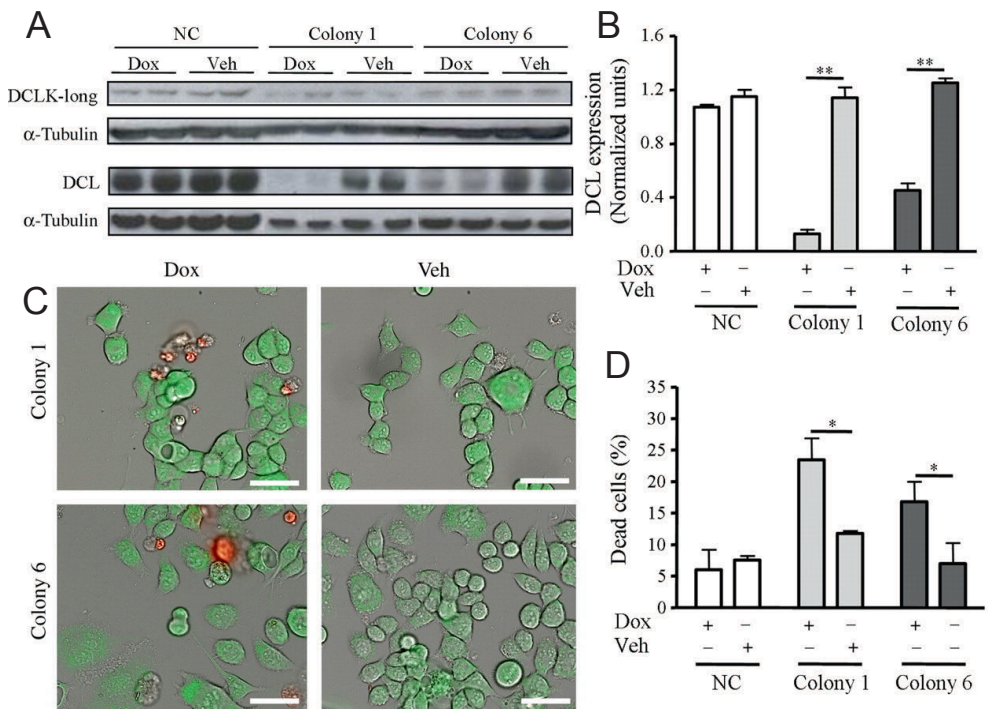

Figure 6 - DCL knockdown leads to cell death in a neuroblastoma stable cell line with an inducible shRNA expression. (A) Western blotting results of DCL, DCLK-long, and α-tubulin expression in N1E-115 stable cell line with a doxycycline (Dox)-inducible shRNA expression against DCL. An effect on DCL but not on DCLK-long expression was detected. Description of the development of this stable neuroblastoma cell line is provided in Materials and methods. The cells were treated with 1 mg/ml of doxycycline (Dox) or with vehicle (Veh). In the presence of Dox, a specific shRNA for DCL is expressed, leading to DCL knockdown. (B) Quantification results of DCL expression normalized to α-tubulin. For colony 1 and colony 6, a significant difference in DCL expression was found between cells with the induced knockdown and the cells treated with vehicle. Moreover, compared with the cells that do not present the inducible system (NC), no leakage in DCL knockdown due to shRNA expression was detected. (C and D), Live/dead double staining assays reveal an induction of cell death when DCL knockdown is induced in both colonies 1 and 6. In the negative control, no significant difference was found between cells treated with Dox and Veh. NC, negative control (N1E-115 cells). 20x magnification. Scale bars, 50 mm. Columns, mean of two independent experiments (n=6); bars, S.E.M. *, $P < 0.05$. **, $P < 0.01$.

In agreement with these observations, induction of apoptosis in NB cells by silencing of DCL/DCLK-long was confirmed by several assays. A higher PS translocation to the outer membrane and a higher percentage of cells with membrane damage were observed during the knockdown. Also, a higher

percentage of apoptotic cells were detected by FACS analysis in the knockdown group. Moreover, an increase in caspase-3 activation was detected in these cells as well.

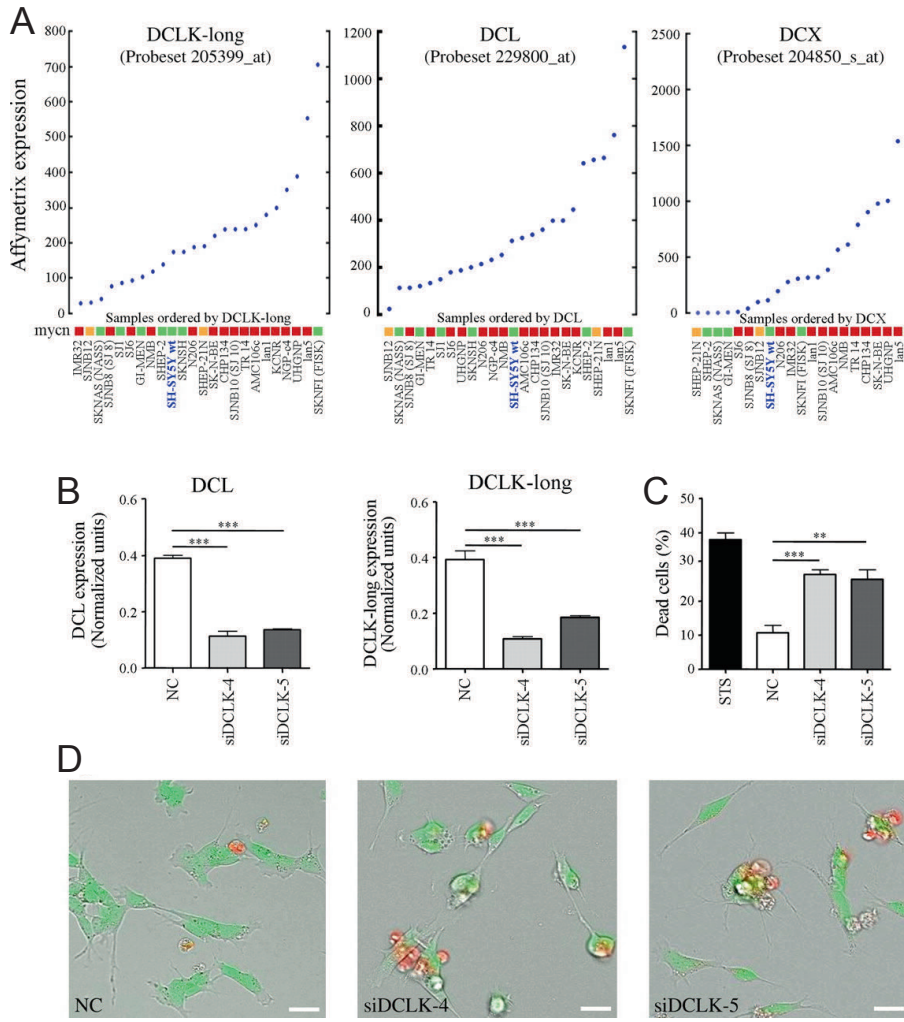

Figure 7 - DCL/DCLK-long knockdown in human SH-SY5Y neuroblastoma cells and cell death studies at 48 h after transfection. (A) Average microarray mRNA expression levels of DCLK-long, DCL, and DCX in several human neuroblastoma cells. SH-SY5Y cells (blue) were selected for further experiments since they have high level of DCL and DCLK-long expression, but low level of DCX expression. mycn: green, single copy; red, amplification; orange: overexpression (SHEP21N) or cMyc amplified (SJNB12). (B) Quantification of DCL and DCLK-long protein expression in human SH-SY5Y neuroblastoma cells 48 h after transfection with siDCLK-4, siDCLK-5 or negative control. A visible knockdown of DCL/DCLK-long was obtained. The expression is normalized to α-tubulin. Western blotting is shown in Supplementary Figure S3. (C and D) Live/dead double staining assay showed an induction of cell death in human neuroblastoma cells with DCL/DCLK-long knockdown. (C) Quantification of dead cells at 48 h after transfection. (D) Overlap of DIC and fluorescent imaging of live/dead double stained SH-SY5Y cells. Viable cells are stained with a cell-permeable green fluorescent cyto-dye, and dead cells are

stained with both cyto-dye (green) and propidium iodide (red). STS, 500 nM staurosporine. NC, cells transfected with AllStars Negative Control siRNA from Qiagen. 20x magnification. Scale bars, 50 mm. Columns, mean of two independent experiments (n=6); bars, S.E.M. **, $P < 0.01$. ***, $P < 0.001$.

We have previously shown that cells transfected with siDCL-3 present more disruption of the mitotic spindles (Vreugdenhil et al., 2007), and we identified a higher percentage of cell death in cells transfected with siDCL-3 than in those transfected with siDCL-2. Therefore, our present and previous results suggest that the effectiveness of inducing apoptosis in NB cells may be directly correlated with the level of disruption of mitotic spindles. Previously, we and others have shown that silencing (Shu et al., 2006; Vreugdenhil et al., 2007) or overexpression (Fitzsimons et al., 2008; Santra et al., 2009; Santra et al., 2006; Shu et al., 2006) of MAPs of the DCX family leads to inhibition of cell proliferation. As shown previously, an imbalance in the expression levels of DCL, DCLK-long, or DCX results in aberrant spindle morphology, leading to a comparable disruption in the mitotic progression (Shu et al., 2006; Vreugdenhil et al., 2007). Consistent with this, a link between mitotic arrest due to disruption of mitotic spindles and apoptosis has been described, involving the activation of the pro-apoptotic gene Bax (Bhalla, 2003). In our experiments, Bax was up-regulated after DCL/DCLK-long knockdown. In addition, survivin (Bric5) was found down-regulated, suggesting mitotic spindle catastrophe leading to apoptosis (Bhalla, 2003).

An alternative explanation for our results might be that intracellular transport of signaling proteins might have been disrupted by DCL/DCLK-long knockdown, which lead the cell toward apoptosis. We have previously shown that DCL regulates GR microtubule-guided intracellular transport in mouse NB cells and in brain neuroblasts (Fitzsimons et al., 2008). GR is known to be transported to mitochondria where it activates specific responsive genes (Solakidi et al., 2007). Interestingly, mitochondria were the most affected cell components after DCL/DCLK-long knockdown. Furthermore, we found in human NBs a significant correlation between DCL and genes related with mitochondria activity. Interestingly, the relation between DCL and mitochondria function might not be independent from the role of DCL in microtubule stabilization. Mitochondria transport is known to be along microtubules (Morris and Hollenbeck, 1995), and connection between microtubules and mitochondrial apoptotic machinery has been proposed (Esteve et al., 2007).

In In conclusion, we identified high expression of DCLK-derived MAPs in human NBs. We demonstrate for the first time at the gene expression level and by several cell death assays that DCL/DCLK-long knockdown induces profound apoptosis in mouse and human NB cells. Therefore, our results suggest that the MAPs DCL and DCLK-long, which are specifically expressed in proliferative neuroblasts, might be targets for the treatment of NB.

DECLARATION OF INTEREST

The authors declare that there is no conflict of interest that could be perceived as prejudicing the impartiality of the research reported.

FUNDING

This work was supported by Top Institute Pharma, The Netherlands.

ACKNOWLEDGEMENTS

The authors thank Saskia Burm, Theo Schouten, Jessica Kamphorst, and Ethan den Boer for technical assistance.

REFERENCES

Abramoff MD, Magelhaes PJ, Ram SJ (2004) Image Processing with ImageJ. Biophotonics International 11: 36-42.

Anthony TE, Klein C, Fishell G, Heintz N (2004) Radial glia serve as neuronal progenitors in all regions of the central nervous system. Neuron 41: 881-890.

Bai J, Ramos RL, Ackman JB, Thomas AM, Lee RV, LoTurco JJ (2003) RNAi reveals doublecortin is required for radial migration in rat neocortex. Nat Neurosci 6: 1277-1283.

Balcer-Kubiczek EK, Attarpour M, Jiang J, Kennedy AS, Suntharalingam M (2006) Cytotoxicity of docetaxel (Taxotere) used as a single agent and in combination with radiation in human gastric, cervical and pancreatic cancer cells. Chemotherapy 52: 231-240.

Benjamini Y, Hochberg Y (1995) Controlling the false discovery rate: a practical and powerful approach to multiple testing. Journal of the Royal Statistical Society 52: 231-240.

Berger J, Berger S, Tuoc TC, D'Amelio M, Cecconi F, Gorski JA, Jones KR, Gruss P, Stoykova A (2007) Conditional activation of Pax6 in the developing cortex of transgenic mice causes progenitor apoptosis. Development 134: 1311-1322.

Bhalla KN (2003) Microtubule-targeted anticancer agents and apoptosis. Oncogene 22: 9075-9086.

Bhat KM, Setaluri V (2007) Microtubule-associated proteins as targets in cancer chemotherapy. Clin Cancer Res 13: 2849-2854.

Boekhoorn K, Sarabdjitsingh A, Kommerie H, de Punder K, Schouten T, Lucassen PJ, Vreugdenhil E (2008) Doublecortin (DCX) and doublecortin-like (DCL) are differentially expressed in the early but not late stages of murine neocortical development. J Comp Neurol 507: 1639-1652.

Brodeur GM (2003) Neuroblastoma: biological insights into a clinical enigma. Nat Rev Cancer 3: 203-216.

Burgess HA, Reiner O (2000) Doublecortin-like kinase is associated with microtubules in neuronal growth cones. Mol Cell Neurosci 16: 529-541.

Burgess HA, Reiner O (2001) Cleavage of doublecortin-like kinase by calpain releases an active kinase fragment from a microtubule anchorage domain. J Biol Chem 276: 36397-36403.

Burgess HA, Reiner O (2002) Alternative splice variants of doublecortin-like kinase are differentially expressed and have different kinase activities. J Biol Chem 277: 17696-17705.

Castel V, Grau E, Noguera R, Martinez F (2007) Molecular biology of neuroblastoma. Clin Transl Oncol 9: 478-483.

Coquelle FM, Levy T, Bergmann S, Wolf SG, Bar-El D, Sapir T, Brody Y, Orr I, Barkai N, Eichele G, et al. (2006) Common and divergent roles for members of the mouse DCX superfamily. Cell Cycle 5: 976-983.

Deuel TA, Liu JS, Corbo JC, Yoo SY, Rorke-Adams LB, Walsh CA (2006) Genetic interactions between doublecortin and doublecortin-like kinase in neuronal migration and axon outgrowth. Neuron 49: 41-53.

Dijkmans TF, van Hooijdonk LW, Schouten TG, Kamphorst JT, Vellinga AC, Meerman JH, Fitzsimons CP, de Kloet ER, Vreugdenhil E (2008) Temporal and functional dynamics of the transcriptome during nerve growth factor-induced differentiation. J Neurochem 105: 2388-2403.

Don S, Verrills NM, Liaw TY, Liu ML, Norris MD, Haber M, Kavallaris M (2004) Neuronal-associated microtubule proteins class III beta-tubulin and MAP2c in neuroblastoma: role in resistance to microtubule-targeted drugs. Mol Cancer Ther 3: 1137-1146.

Engels BM, Schouten TG, van Dullemen J, Gosens I, Vreugdenhil E (2004) Functional differences between two DCLK splice variants. Brain Res Mol Brain Res 120: 103-114.

Esteve MA, Carre M, Braguer D (2007) Microtubules in apoptosis induction: are they necessary? Curr Cancer Drug Targets 7: 713-729.

Fitzsimons CP, Ahmed S, Wittevrongel CF, Schouten TG, Dijkmans TF, Scheenen WJ, Schaaf MJ, de Kloet ER, Vreugdenhil E (2008) The microtubule-associated protein doublecortin-like regulates the transport of the glucocorticoid receptor in neuronal progenitor cells. Mol Endocrinol 22: 248-262.

Francis F, Koulakoff A, Boucher D, Chafey P, Schaar B, Vinet MC, Friocourt G, McDonnell N, Reiner O, Kahn A, et al. (1999) Doublecortin is a developmentally regulated, microtubule-associated protein expressed in migrating and differentiating neurons. Neuron 23: 247-256.

Friocourt G, Koulakoff A, Chafey P, Boucher D, Fauchereau F, Chelly J, Francis F (2003) Doublecortin functions at the extremities of growing neuronal processes. Cereb Cortex 13: 620-626.

Gleeson JG, Lin PT, Flanagan LA, Walsh CA (1999) Doublecortin is a microtubule-associated protein and is expressed widely by migrating neurons. Neuron 23: 257-271.

Green DR, Reed JC (1998) Mitochondria and apoptosis. Science 281: 1309-1312.

Holland EC (2001) Progenitor cells and glioma formation. Curr Opin Neurol 14: 683-688.

Jogi A, Ora I, Nilsson H, Lindeheim A, Makino Y, Poellinger L, Axelson H, Pahlman S (2002) Hypoxia alters gene expression in human neuroblastoma cells toward an immature and neural crest-like phenotype. Proc Natl Acad Sci U S A 99: 7021-7026.

Jordan MA, Thrower D, Wilson L (1992) Effects of vinblastine, podophyllotoxin and nocodazole on mitotic spindles. Implications for the role of microtubule dynamics in mitosis. J Cell Sci 102 (Pt 3): 401-416.

Koizumi H, Tanaka T, Gleeson JG (2006) Doublecortin-like kinase functions with doublecortin to mediate fiber tract decussation and neuronal migration. Neuron 49: 55-66.

Konishi Y, Lehtinen M, Donovan N, Bonni A (2002) Cdc2 phosphorylation of BAD links the cell cycle to the cell death machinery. Mol Cell 9: 1005-1016.

Kruidering M, Schouten T, Evan GI, Vreugdenhil E (2001) Caspase-mediated cleavage of the Ca2+/calmodulin-dependent protein kinase-like kinase facilitates neuronal apoptosis. J Biol Chem 276: 38417-38425.

Lenka N, Vijayasarathy C, Mullick J, Avadhani NG (1998) Structural organization and transcription regulation of nuclear genes encoding the mammalian cytochrome c oxidase complex. Prog Nucleic Acid Res Mol Biol 61: 309-344.

Lin PT, Gleeson JG, Corbo JC, Flanagan L, Walsh CA (2000) DCAMKL1 encodes a protein kinase with homology to doublecortin that regulates microtubule polymerization. J Neurosci 20: 9152-9161.

Lobert S, Ingram JW, Correia JJ (1999) Additivity of dilantin and vinblastine inhibitory effects on microtubule assembly. Cancer Res 59: 4816-4822.

Lopez E, Ferrer I (2000) Staurosporine- and H-7-induced cell death in SH-SY5Y neuroblastoma cells is associated with caspase-2 and caspase-3 activation, but not with activation of the FAS/FAS-L-caspase-8 signaling pathway. Brain Res Mol Brain Res 85: 61-67.

Mamelak AJ, Kowalski J, Murphy K, Yadava N, Zahurak M, Kouba DJ, Howell BG, Tzu J, Cummins DL, Liegeois NJ, et al. (2005) Downregulation of NDUFA1 and other oxidative phosphorylation-related genes is a consistent feature of basal cell carcinoma. Exp Dermatol 14: 336-348.

Maris JM, Hogarty MD, Bagatell R, Cohn SL (2007) Neuroblastoma. Lancet 369: 2106-2120.

Maris JM, Matthay KK (1999) Molecular biology of neuroblastoma. J Clin Oncol 17: 2264-2279.

Molenaar JJ, Ebus ME, Koster J, van Sluis P, van Noesel CJ, Versteeg R, Caron HN (2008) Cyclin D1 and CDK4 activity contribute to the undifferentiated phenotype in neuroblastoma. Cancer Res 68: 2599-2609.

Morris RL, Hollenbeck PJ (1995) Axonal transport of mitochondria along microtubules and F-actin in living vertebrate neurons. J Cell Biol 131: 1315-1326.

Nakai K, Horton P (1999) PSORT: a program for detecting sorting signals in proteins and predicting their subcellular localization. Trends Biochem Sci 24: 34-36.

Nazarewicz RR, Zenebe WJ, Parihar A, Larson SK, Alidema E, Choi J, Ghafourifar P (2007) Tamoxifen induces oxidative stress and mitochondrial apoptosis via stimulating mitochondrial nitric oxide synthase. Cancer Res 67: 1282-1290.

Nutt LK, Pataer A, Pahler J, Fang B, Roth J, McConkey DJ, Swisher SG (2002) Bax and Bak promote apoptosis by modulating endoplasmic reticular and mitochondrial Ca2+ stores. J Biol Chem 277: 9219-9225.

Poomthavorn P, Wong SH, Higgins S, Werther GA, Russo VC (2009) Activation of a prometastatic gene expression program in hypoxic neuroblastoma cells. Endocr Relat Cancer 16: 991-1004.

Puigvert JC, de Bont H, van de Water B, Danen EH (2010) High-throughput live cell imaging of apoptosis. Curr Protoc Cell Biol Chapter 18: Unit 18 10 11-13.

Puigvert JC, Huveneers S, Fredriksson L, op het Veld M, van de Water B, Danen EHJ (2009) Cross-talk between integrins and oncogenes modulates chemosensitivity. Mol Pharmacol 75: 947-955.

Reiner O, Coquelle FM, Peter B, Levy T, Kaplan A, Sapir T, Orr I, Barkai N, Eichele G, Bergmann S (2006) The evolving doublecortin (DCX) superfamily. BMC Genomics 7: 188.

Santra M, Santra S, Roberts C, Zhang RL, Chopp M (2009) Doublecortin induces mitotic microtubule catastrophe and inhibits glioma

cell invasion. J Neurochem 108: 231-245.

Santra M, Zhang X, Santra S, Jiang F, Chopp M (2006) Ectopic doublecortin gene expression suppresses the malignant phenotype in glioblastoma cells. Cancer Res 66: 11726-11735.

Schenk GJ, Engels B, Zhang YP, Fitzsimons CP, Schouten T, Kruidering M, de Kloet ER, Vreugdenhil E (2007) A potential role for calcium / calmodulin-dependent protein kinase-related peptide in neuronal apoptosis: in vivo and in vitro evidence. Eur J Neurosci 26: 3411-3420.

Seibler J, Kleinridders A, Kuter-Luks B, Niehaves S, Bruning JC, Schwenk F (2007) Reversible gene knockdown in mice using a tight, inducible shRNA expression system. Nucleic Acids Res 35: e54.

Shu T, Tseng HC, Sapir T, Stern P, Zhou Y, Sanada K, Fischer A, Coquelle FM, Reiner O, Tsai LH (2006) Doublecortin-like kinase controls neurogenesis by regulating mitotic spindles and M phase progression. Neuron 49: 25-39.

Simon R, Lam A (2006) BRB Array Tools Users Guide, version 3.2. Biometric Research Branch, National Cancer Institute http://linus.nci.nih.gov/brb.

Solakidi S, Psarra AM, Sekeris CE (2007) Differential distribution of glucocorticoid and estrogen receptor isoforms: localization of GRbeta and ERalpha in nucleoli and GRalpha and ERbeta in the mitochondria of human osteosarcoma SaOS-2 and hepatocarcinoma HepG2 cell lines. J Musculoskelet Neuronal Interact 7: 240-245.

Tang XX, Zhao H, Kung B, Kim DY, Hicks SL, Cohn SL, Cheung NK, Seeger RC, Evans AE, Ikegaki N (2006) The MYCN enigma: significance of MYCN expression in neuroblastoma. Cancer Res 66: 2826-2833.

Tuy FP, Saillour Y, Kappeler C, Chelly J, Francis F (2008) Alternative transcripts of Dclk1 and Dclk2 and their expression in doublecortin knockout mice. Dev Neurosci 30: 171-186.

Valentijn LJ, Koster J, Versteeg R (2006) Read-through transcript from NM23-H1 into the neighboring NM23-H2 gene encodes a novel protein, NM23-LV. Genomics 87: 483-489.

Vreugdenhil E, Datson N, Engels B, de Jong J, van Koningsbruggen S, Schaaf M, de Kloet ER (1999) Kainate-elicited seizures induce mRNA encoding a CaMK-related peptide: a putative modulator of kinase activity in rat hippocampus. J Neurobiol 39: 41-50.

Vreugdenhil E, Engels B, Middelburg R, van Koningsbruggen S, Knol J, Veldhuisen B, de Kloet ER (2001) Multiple transcripts generated by the DCAMKL gene are expressed in the rat hippocampus. Brain Res Mol Brain Res 94: 67-74.

Vreugdenhil E, Kolk SM, Boekhoorn K, Fitzsimons CP, Schaaf M, Schouten T, Sarabdjitsingh A, Sibug R, Lucassen PJ (2007) Doublecortin-like, a microtubule-associated protein expressed in radial glia, is crucial for neuronal precursor division and radial process stability. Eur J Neurosci 25: 635-648.

Wright GW, Simon RM (2003) A random variance model for detection of differential gene expression in small microarray experiments. Bioinformatics 19: 2448-2455.

Yamaguchi H, Wang HG (2002) Bcl-XL protects BimEL-induced Bax conformational change and cytochrome C release independent of interacting with Bax or BimEL. J Biol Chem 277: 41604-41612.

SUPPLEMENTARY DATA

Supplementary figures

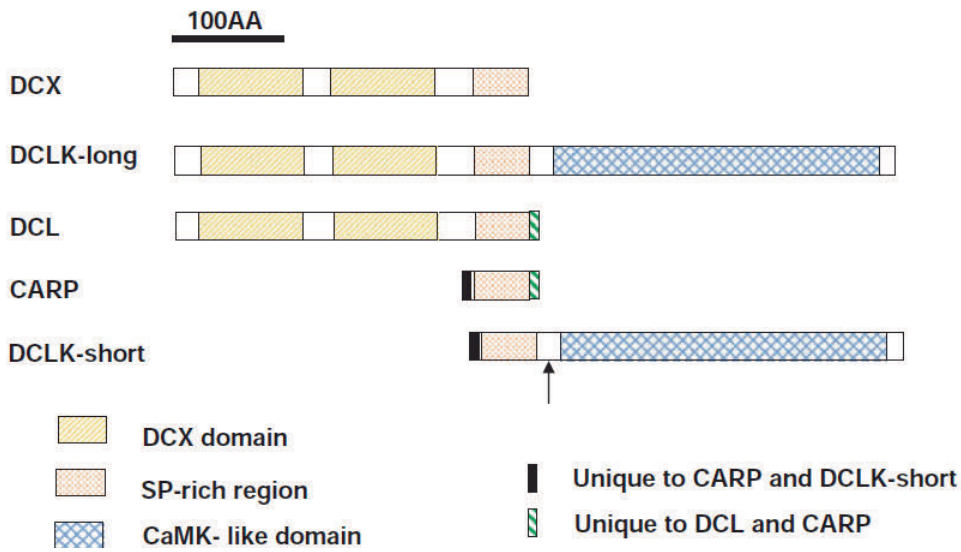

Supplementary Figure S1 – Doublecortin (DCX) and the main proteins encoded by the doublecortin-like kinase (DCLK) gene: DCLK-long, Doublecortin-like (DCL), calcium/calmodulin-dependent protein kinase (CaMK)-related peptide (CARP) and DCLK-short. DCLK-long and DCL contain two DCX domains (Burgess and Reiner 2000; Gleeson, et al. 1999; Vreugdenhil et al. 2007). DCLK-long and DCLK-short contain a CaMK-like domain (Schenk et al. 2007). DCLK-short is abundantly expressed in limbic structures of the adult brain (Burgess and Reiner 2002; Engels, et al. 2004; Vreugdenhil, et al. 2001). CARP transcript lacks both DCX and CaMK-like domains (Vreugdenhil, et al. 1999). CARP expression is below detection levels under normal conditions. In contrast, CARP mRNA is highly up-regulated by kainate-induced seizures in the hippocampus (Vreugdenhil, et al. 1999). Adapted figure (Schenk, et al. 2007).

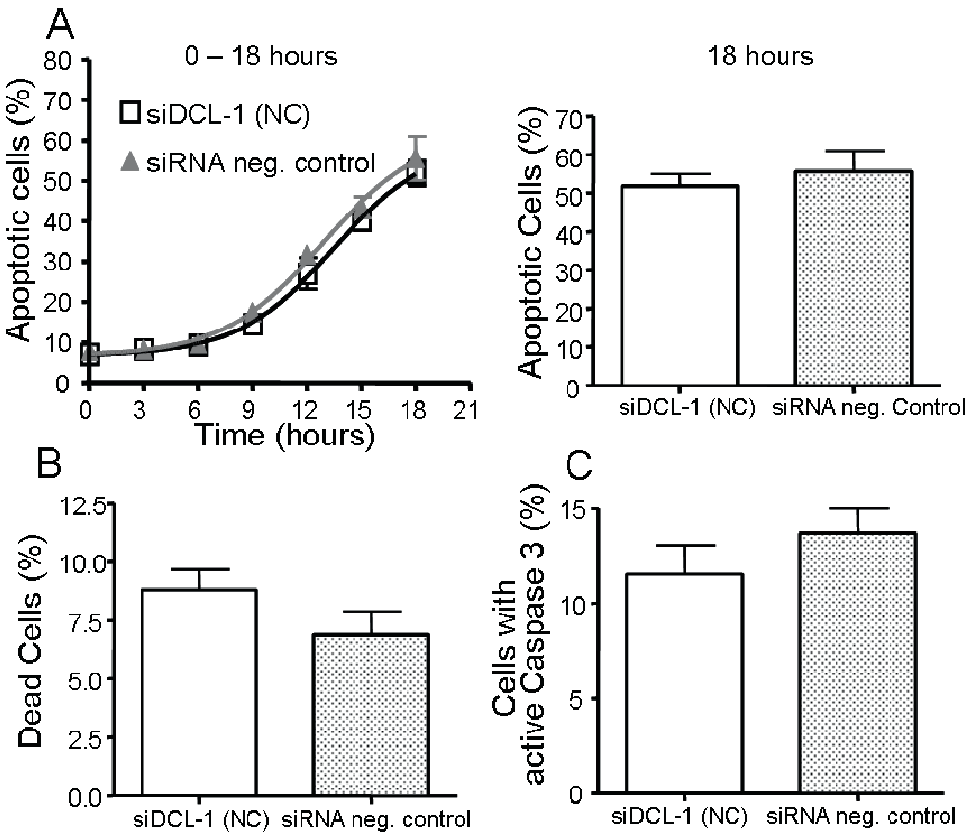

Supplementary Figure S2 – Comparison of results obtained with siDCL-1 and a commercial negative control siRNA. A, time lapse imaging of phosphatidyl-serine translocation at different time points after starting the assay (0 – 18 hours and 18 hours). B, Percentage of dead cells quantified by using Lve/Dead doublestaining assay. C, Percentage of cells with active caspase 3. No significant differences were detected using the two control siRNAs. siDCL-1, no effective siRNA. siRNA neg. control, AllStars negative control siRNA from Qiagen.

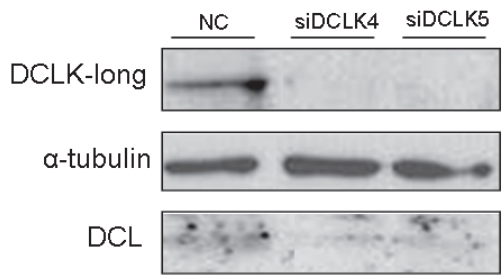

Supplementary Figure S3 – Western blotting results of DCL, DCLK-long and α-tubulin expression in human SH-SY5Y neroblastoma cells 48 hours after transfection. The protein quantification and normalization to α-tubulin is presented in Figure 7B. Cells were transfected with siDCLK-4, siDCLK-5 or NC, commercial negative control siRNA (AllStars negative control siRNA from Qiagen).

Supplementary videos can be found at http://dx.doi.org/10.1677/ERC-09-0301

Legends:

Supplementary video 1A – Time lapse imaging of phosphatidyl-serine translocation in N1E-115 neuroblastoma cells 48 hours after transfection. Negative control; Images were taken at 30 minutes interval. Overlap of DIC and fluorescent imaging was used in the different assays. 20x magnification.

Supplementary video 1B – Time lapse imaging of phosphatidyl-serine translocation in N1E-115 neuroblastoma cells 48 hours after transfection. Cells transfected with siDCL-2; Images were taken at 30 minutes interval. Overlap of DIC and fluorescent imaging was used in the different assays. 20x magnification.

Supplementary video 1C – Time lapse imaging of phosphatidyl-serine translocation in N1E-115 neuroblastoma cells 48 hours after transfection. siDCL-3 transfected cells. Images were taken at 30 minutes interval. Overlap of DIC and fluorescent imaging was used in the different assays. 20x magnification.

Supplementary tables

Supplementary Table S1 – 10 gene ontology categories that are most significantly enriched for genes that correlated with DCLK-long (*P* < 0.01). GO path, gene ontology path. R#, number of genes in the GO category. #, number of significant correlated genes in the GO cluster. GOID, Gene Ontology identification. Desc, description.

GoPath	R#	#	p value	Goid-Desc	Gene Symbols
1.5.25.9.5.7	182	39	1.10E-12	7017:microtubule-based process	RANBP9, TUBB3, TUBB2C, TACC3, TPPP, KIF3A, DYNC1I1, DYNC1L2, TUBB, KIFAP3, KIF1B, RNF19A, TUBG2, APBA1, APC, KIF3C, KIF5C, KLC1, MAP1B, MAP2, MAP4, MAPT, PAFAH1B1, STMN3, GTSE1, PRKCZ, KIF15, DST, AURKA, TUBB2A, UCHL1, KIF18A, UXT, HOOK3, TUBB6, DOCK7, KIFC2, KIF23, KIF14
3.2.14.11	126	29	6.00E-11	43005: neuron projection	CRMP1, NRSN1, DPYSL2, MYCBP2, FREQ, BACE1, ATXN10, GAP43, DNM3, ANK3, KCNMA1, KIF5C, KLC1, MAPT, MYO5A, NCAM1, NRCAM, NSF, PAK1, TRAPPC4, PPP1R9A, MAGEE1, SNAP25, STX3, UCHL1, PSD2, DOCK7, CDK5R1, DNER
3.11.4.0.13.6.1	208	40	1.40E-10	5874: microtubule	TUBB3, TUBB2C, APPBP2, KIF3A, DNM1, DYNC1I1, DYNC1I2, DYNC1LI2, TUBB, KIF1B, NEIL2, DNM3, TUBG2, SHROOM2, KIF3C, KIF5C, KLC1, MAP1B, MAP2, MAP4, MAP6, MAPT, PAFAH1B1, GTSE1, NDE1, KIF15, FAM110C, TUBB2A, NDEL1, MAP1LC3B, KIF18A, KATNAL1, HOOK3, MAP1LC3A, TUBB6, CDC16, KIFC2, KIF23, CDC2, KIF14
3.11.4.0.13.6	408	64	1.90E-10	15630: microtubule cytoskeleton	RANBP9, TUBB3, TUBB2C, APPBP2, SPIN1, EMILIN1, KIF3A, AKAP11, DNM1, DYNC1I1, DYNC1I2, DYNC1LI2, TUBB, CEP152, MYCBP2, KIF1B, NEIL2, RNF19A, DNM3, TUBG2, BBS9, APC, SHROOM2, KIF3C, KIF5C, KLC1, KRT18, MAP1B, MAP2, MAP4, MAP6, MAPT, MARK1, MYO5A, NEK2, NPM1, PAFAH1B1, DCTN4, GTSE1, NDE1, PPP2CA, PRKAR2B, KIF15FAM110C, DST, AURKA, BUB1, TUBB2A, NDEL1, MAP1LC3B, KIF18A, KATNAL1, UXT, HOOK3, MAP1LC3A, TUBB6, CDC16, KIFC2, CCNB2, AURKB, KIF23, PDE4DIP, CDC2, KIF14
3.2.41.7	24	10	1.70E-09	30426: growth cone	NRSN1, ERC2, APBB1, MAPT, MYO5A, PAK1, SNAP25, STX3, DOCK7, CDK5R1
1.5.25.9.5.7.9	91	22	3.20E-09	7018: microtubule-based movement	TUBB3, TUBB2C, KIF3A, DYNC1I1, TUBB, KIF1B, APBA1, KIF3C, KIF5C, KLC1, PAFAH1B1, KIF15, DST, TUBB2A, UCHL1, KIF18A, UXT, TUBB6, KIFC2, KIF23, KIF14
3.2.41	25	10	5.20E-09	30427: site of polarized growth	NRSN1, ERC2, APBB1, MAPT, MYO5A, PAK1, SNAP25, STX3, DOCK7, CDK5R1

GoPath	R#	#	p value	Goid-Desc	Gene Symbols
3.8.1.337.3	17	8	7.50E-09	33176: proton-transporting V-type ATPase complex	ATP6V0E2, ATP6V1H, ATP6V1A, ATP6V1B2, ATP6V1C1, ATPV0B, ATP6V1G2, ATP6V0D1
1.5.25.9.5	439	64	1.00E-08	7010: cytoskeleton organization and biogenesis	RANBP9, TUBB3, TUBB2C, CORO2B, TACC3, TPPP, KIF3A, PACSIN2, DYNC1I1, DYNC1I2, TBB, EPB41L1, EPB49, ABLIM3, KIFAP3, MAST1, MYCBP2, ARHGAP26, KIFB, RNF19A, TUBG2, ANK3, CXCL1, APBA1, APC, SHROOM2, KIF3C, KIF5C, KLC1, KRT8, MAP1B, MAP2, MAP4, MAPT, MARK1, MYO5A, PAFAH1B1, PAK1, STMN3, GTSE1, PPP1R9A, PRKCZ, FMN2, KIF15, RALA, SGCB, DST, AURKA, TUBB2A, UCHL1, KIF18A, UXT, HOOK3, ABL1M2, TUBB6, DOCK7, FHDC1, KIFC2, INA, KIF23, PDE4DIP, MTSS1, KIF14, CDC42
1.5.25.9	710	92	1.10E-08	6996: organelle organization and biogenesis	RANBP9, SMC4, OPTN, TUBB3, TUBB2C, CORO2B, TACC3, PTTG2, TPPP, KIF3A, PACSIN2, DYNC1I1, DYNC1I2, TUBB, EPB41L1, EPB49, ABLIM3, KIFAP3, MAST1, MYCBP2, ARHGAP26, KIF1B, RNF19A, PTTG3, TUBG2, ANK3, SLC25A4, CXCL1, HMGB2, APBA1, APC, HSPA1L, SHROOM2, KIF3C, KIF5C, KLC1, KRT8, MAP1B, MAP2, MAP4, MAPT, MARK1, MYO5A, NPM1, PAFAH1B1, PAK1, CALY, STMN3, ACTL6B, GTSE1, ATP6V1H, PEX14, TERF2IP, NDE1, PPP1R9A, PRKCZ, FMN2, KIF15, RALA, RPLP0, MOAP1, NCAPG, SGCB, DST, AURKA, TERF2, TP53, TUBB2A, UCHL1, PIF1, KIF18A, UXT, HOOK3, ABLIM2, MAP1LC3A, TUBB6, DOCK7, FHDC1, CAV2, TNKS, PEX11B, KIFC2, INA, COPB2, KIF23, VPS4B, PDE4DIP, MTSS1, SNAP91, NCAPD2, KIF14, CDC42

Supplementary Table S2 – 10 gene ontology categories that are most significantly enriched for genes that correlated with DCL ($P < 0.01$). GO path, gene ontology path. R#, number of genes in the GO category. #, number of significant correlated genes in the GO cluster. GOID, Gene Ontology identification. Desc, description.

GoPath	R#	#	p value	Goid-Desc	Gene Symbols
3.11.3.0.12.0.14	106	40	3.50E-48	44455: mitochondrial membrane part	TIMM23, TIMM17A, ATP5H, ATP5L, NDUFA11, COX7B, COX15, TIMM13, TIMM10, TIMM8B, UQCRQ, TOMM5, NDUFA1, NDUFA2, NDUFA3, NDUFA6, NDUFA7, NDUFA8, NDUFAB1,NDUFB1, NDUFB9, NDUFB10, NDUFC2, NDUFS4, NDUFS6, CISD2, OPA1, ATP5C1, ATP5F1, ATP5G1, ATP5J, ATP50, CYCS, NDUFA12, UQCRFS1, COX7A2L, TOMM20, TOMM70A
3.11.3.0.12	952	143	9.40E-42	5739: mitochondrion	Over 100 entries
3.11.3.0.12.0	341	74	8.40E-41	44429: mitochondrial part	TIMM23, TIMM17A, ATP5H, ATP5L, MRPL3, SFXN4, NDUFA11, CHCHD4, COX6B1, COX7B, COX15, TIMM8A, FH, FKBP8, TIMM13, TIMM10, TIMM8B, UQCRQ, COQ2, GOT2, NR3C1, HSPD1, TOMM5, ME2, NDUFA1, NDUFA2, NDUFA3, NDUFA6, NDUFA7, NDUFA8, NDUFAB1, NDUFB1, NDUFB8, NDUFB9, NDUFB10, NDUFC2, NDUFS4, NDUFS6, CISD2, OAT, OPA1, ATP5C1, MRPS18C, MRPL27, ATP5F1, ATP5G1, PDHA1, PDK1, COQ3, ATP5J, PIN4, ATP50, MRPL39, CYCS, MRPS18A, OGDHL, NDUFA12, MRPL47, MRPL12, MRPS25, MRPL36, SOD1, UQCRC2, UQCRFS1, MRP63, NARS2, GRPEL1, PDHX, SUCLG1, DNAJA3, COX7A2L, TOMM20, TOMM70A
3.2.29.12.87	939	138	1.50E-38	5739: mitochondrion	Over 100 entries
3.11.3.0.12.0.14.16	60	23	2.50E-28	5746: mitochondrion respiratory chain	NDUFA11, COX7B, COX15, UQCRQ, NDUFA1, NDUFA2, NDUFA3, NDUFA6, NDUFA7, NDUFA8, NDUFAB1, NDUFB1, NDUFB8, NDUFB9, NDUFB10, NDUFC2, NDUFS4, NDUFS6, CYCS, NDUFA12, UQCRC2, UQCRFS1, COX7A2L
2.4.26.37.0	36	16	1.20E-23	3954: NADH dehydrogenase activity	NDUFA1, NDUFA2, NDUFA3, NDUFA6, NDUFA7, NDUFA8, NDUFAB1, NDUFB1, NDUFB8, NDUFB9, NDUFB10, NDUFC2, NDUFS4, NDUFS6, NDUFA12, NDUFAF2
2.4.26.37.0.0	36	16	1.20E-23	50136: NADH dehydrogenase (quinine) activity	NDUFA1, NDUFA2, NDUFA3, NDUFA6, NDUFA7, NDUFA8, NDUFAB1, NDUFB1, NDUFB8, NDUFB9, NDUFB10, NDUFC2, NDUFS4, NDUFS6, NDUFA12, NDUFAF2
2.4.26.37.0.0.1	36	16	1.20E-23	8137: NADH dehydrogenase (ubiquinone) activity	NDUFA1, NDUFA2, NDUFA3, NDUFA6, NDUFA7, NDUFA8, NDUFAB1, NDUFB1, NDUFB8, NDUFB9, NDUFB10, NDUFC2, NDUFS4, NDUFS6, NDUFA12, NDUFAF2

GoPath	R#	#	p value	Goid-Desc	Gene Symbols
2.4.26.37.8.1	36	16	1.20E-23	8137: NADH dehydrogenase (ubiquinone) activity	NDUFA1, NDUFA2, NDUFA3, NDUFA6, NDUFA7, NDUFA8, NDUFAB1, NDUFB1, NDUFB8, NDUFB9, NDUFB10, NDUFC2, NDUFS4, NDUFS6, NDUFA12, NDUFAF2
2.4.26.37.8	41	16	3.50E-20	16655: oxidoreductase activity, acting on NADH or NADPH, quinine or similar compound as acceptor	NDUFA1, NDUFA2, NDUFA3, NDUFA6, NDUFA7, NDUFA8, NDUFAB1, NDUFB1, NDUFB8, NDUFB9, NDUFB10, NDUFC2, NDUFS4, NDUFS6, NDUFA12, NDUFAF2
3.8.0	396	62	1.30E-19	30529: ribonucleoprotein complex	MRPS31, SMNDC1, RPP30, UTP14A, MRPS30, TXNL4A, LSM6, MRPL3, MRPL54, DHX15, DKC1, EIF2S1, RPL22L1, FRG1, LSM4, RSL1D1, LSM3, MRPL15, MRPL22, HNRNPC, HNRNPH3, MRPS18C, UTP18, RPL26L1, MRPL30, MRPL27, MRPL48, PPIL1, LSM7, PPIL3, MRPL39, MRPS18A, NHP2, PSMA1, MRPL47, SRPRB, RPL12, MRPL23, RPL27A, RPL36L, RPL36A, MRPL12, RPS3, SFRS1, MRPS25, MRPL14, MRPS6, MRPL36, SNRPD1, SNRPD2, SNRPG, SRP72, SSB, TEP1, U2AF1, MRP63, SNRNP25, GEMIN6, SIP1, PRPF4B, RPL14, UTP14C

Supplementary Table S3 – Prediction of subcellular localization of human and mouse DCL and DCLK-long based in the amino acid sequence (PSORT II).

Subcellular localization	***Mus musculus***		***Homo sapiens***	
Protein	**DCL** (NP_001104523.1)	**DCLK-long** (NP_064362.1)	**DCL** (NP_001092904)	**DCLK-long** (NP_001035350.2)
Nuclear	73.90%	39.10%	47.80%	34.80%
Cytoplasmic	13.00%	17.40%	17.40%	17.40%
Mitochondrial	13.00%	13.00%	17.40%	17.40%
Golgi	0%	13.00%	4.30%	13.00%
Cytoskeletal	0%	4.30%	4.30%	4.30%
Vesicles of secretory system	0%	4.30%	8.70%	4.30%
Extracellular, including cell wall	0%	4.30%	0%	4.30%
Plasma membrane	0%	4.30%	0%	4.30%

Supplementary Table S4 – Fold change and function of the 663 differently expressed genes in both comparisons: Negative control (NC) versus siDCL-2 groups and negative control versus siDCL-3. $P < 0.001$ and FDR < 0.015.

ProbeID	Gene Symbol	Fold change NC vs. siDCL-2	Fold change NC vs. siDCL-3	Function (Panther)
516618	Sdfr2	6.37	3.32	Molecular function unclassified
449813	Pax6	6.17	5.17	Transcription factor| Homeobox transcription factor; Nucleic acid binding| Other DNA-binding protein
873028	Mt3	6.09	4.82	Molecular function unclassified
725017	Ndufa7	5.41	4.25	Molecular function unclassified
865155	LOC554362	5.39	5.37	
635397		5.18	5.17	
918134	Bola2	5.18	4.63	Molecular function unclassified
678434	2010107H07Rik	5.17	4.93	
897494	LOC632400| LOC625492	5.12	5.06	Nucleic acid binding| Ribosomal protein
583790	Anapc13	4.94	5.36	
897170	LOC634654| 2010100O12Rik| LOC624701	4.83	5.13	
900218	LOC629182	4.78	5.02	
933033	Atp5e	4.77	4.16	Molecular function unclassified
921671	Son	4.77	5.11	Molecular function unclassified
900702		4.77	4.74	
342192	Ndufa3	4.67	5.10	Molecular function unclassified
907414	1810027O10Rik	4.66	4.62	
916906	Mt1	4.61	3.13	Molecular function unclassified
453149	Dpm3	4.61	4.58	
805956	1110021J02Rik	4.56	3.87	
899481	Rps29	4.52	4.01	Molecular function unclassified
555568	Ndufa1	4.47	4.48	Oxidoreductase
896328	LOC227112	4.47	3.78	Molecular function unclassified
449526	1810035L17Rik	4.47	4.00	Other RNA-binding protein| Nucleic acid binding
908461	Ndufa2	4.40	4.35	Molecular function unclassified
895172	LOC239658	4.39	4.57	Nucleic acid binding| Ribosomal protein
897700	Uqcr|LOC640373| LOC621999	4.37	3.90	Oxidoreductase| Reductase
917278	Mt1	4.36	2.61	Molecular function unclassified
891974	Tomm7	4.33	4.37	Transporter| Other transporter;Transfer/carrier protein| Mitochondrial carrier protein
716278	Ndufa3	4.32	4.86	Molecular function unclassified
916613	Gm1673	4.31	5.56	
365220	2010107E04Rik	4.22	4.09	Molecular function unclassified
797198	Gng8	4.20	5.19	Large G-protein| G-protein| Select regulatory molecule
897264	Pin4	4.16	3.72	Isomerase| Other isomerase
901609	LOC432491	4.13	3.74	Molecular function unclassified
303204	LOC633736| LOC623077	4.12	3.86	Nucleic acid binding| Ribosomal protein
309126	1500034E06Rik	4.10	4.33	Molecular function unclassified
677462	1110001J03Rik	4.08	4.71	
899036	LOC623265| LOC640777	4.07	4.32	Nucleic acid binding| Ribosomal protein
615889	LOC625730| LOC632018	4.03	3.93	mRNA splicing factor| Nucleic acid binding| mRNA processing factor
856341	Pcbd2	4.03	3.32	Lyase| Dehydratase
700699	2310007A19Rik	4.02	4.40	
900375		4.01	3.95	
349481	1110002M09Rik	3.98	4.37	
625011	Tloc1	3.96	3.75	Molecular function unclassified

558410	Cox17	3.94	3.86	Transfer/carrier protein
715000	LOC632183| LOC621893	3.94	3.83	Histone| Nucleic acid binding
480641	Mrpl33	3.92	3.45	
856025	Hist1h4f	3.88	2.75	Histone| Nucleic acid binding
895008	LOC632563| LOC623719	3.88	4.33	Membrane traffic protein| Other membrane traffic protein
505384	Snx30	3.88	3.04	Membrane traffic regulatory protein| Membrane traffic protein
629891	LOC640896| BC024760	3.84	3.88	Molecular function unclassified
896327	LOC627998| LOC632911	3.83	3.67	Molecular function unclassified
891830	LOC636262	3.83	3.94	
751602	LOC623101| LOC633757	3.82	4.00	Nucleic acid binding| Ribosomal protein
335432		3.80	3.56	
895997	LOC623595| LOC632478	3.80	3.53	Molecular function unclassified
510029		3.79	4.08	Molecular function unclassified
898872	Atp5l	3.78	3.42	Molecular function unclassified
808796	Mt2	3.76	2.71	Molecular function unclassified
503614	1190017O12Rik	3.76	3.00	
896997	LOC384953| LOC436081| LOC625336| LOC631575	3.76	3.98	Nucleic acid binding| Ribosomal protein
323268	Gm561	3.69	3.14	
299345	LOC626270	3.69	3.95	Ribosomal protein| Nucleic acid binding
899685	LOC545531| LOC432760| Snrpd2|LOC631370	3.69	3.39	Nucleic acid binding|mRNA processing factor
683066	2310039H08Rik	3.66	3.09	
895253	Rpl36|LOC636594| Atp6v1c2	3.64	3.61	Transporter| Other hydrolase| Nucleic acid binding| Synthase| Ribosomal protein| Cation transporter| ATP synthase; Hydrolase| Hydrogen transporter; Synthase and synthetase
732583	Timm8b	3.64	3.50	Transporter| Other transporter
690372		3.63	3.26	
428201	5830418K08Rik	3.63	2.89	Molecular function unclassified
899864	LOC436233	3.60	3.60	Transcription factor| Transcription cofactor
701966	Ly6g6c	3.60	3.40	
896537		3.59	3.71	Oxidoreductase| Oxidase
929933	Bola1	3.58	3.19	Molecular function unclassified
903930	LOC626569| LOC632898	3.57	3.72	Membrane traffic protein| Other membrane traffic protein
913930	4930517K11Rik	3.57	3.84	Ribosomal protein|Nucleic acid binding
921119	Hint3	3.56	3.48	Nucleic acid binding|Damaged DNA-binding protein
556632	2310009A05Rik	3.56	4.15	
496861	Mrpl52	3.56	3.94	
902257	C330007P06Rik	3.54	3.86	Molecular function unclassified
333496		3.48	4.48	
896424	LOC635161	3.47	3.44	
904530	Atp5l	3.47	3.36	Molecular function unclassified
592095	2310016M24Rik	3.46	3.59	
900376	LOC635999| LOC628161|Pin4	3.46	3.32	Isomerase|Other isomerase
933131	Tceb2	3.45	3.61	Transcription factor|Transcription cofactor
580194	2310009B15Rik	3.45	3.92	Molecular function unclassified
556900	2610019E17Rik	3.45	3.46	

883725	1110020P15Rik	3.44	3.38	Oxidoreductase|Reductase
924567	Hist1h4c|Hist1h4d| Hist1h4i|Hist1h4m| Hist2h4|Hist1h4f| Hist1h4a|Hist1h4b| Hist1h4k|Hist1h4h| Hist1h4j	3.42	2.32	Histone|Nucleic acid binding
893646	LOC638835| LOC622534	3.41	3.47	Nucleic acid binding|Ribosomal protein
896854	Cox7c	3.40	3.46	Oxidoreductase|Oxidase
303657	Arpc1b	3.40	3.44	Other actin family cytoskeletal protein|Cytoskeletal protein| Actin binding cytoskeletal protein
900771	LOC629957| LOC632013|Rps29| LOC627746	3.39	3.52	Molecular function unclassified
355965	Glul	3.37	4.03	Synthetase;Ligase|Synthase and synthetase|Other ligase
901580	LOC629406| LOC633091	3.37	3.64	Membrane traffic protein|Other membrane traffic protein
642051	Aqp11	3.36	3.91	Molecular function unclassified
898913	LOC625052| LOC634664	3.36	3.43	
908765	3110001D03Rik	3.34	2.64	
901679		3.34	3.02	
334316	2410017P09Rik	3.33	3.19	Molecular function unclassified
693304	2610042O14Rik	3.32	2.97	Molecular function unclassified
334457	Tcte3	3.32	3.36	Molecular function unclassified
912694	0910001L09Rik	3.31	3.85	
687981	2310061C15Rik	3.29	2.44	Molecular function unclassified
897650	Snrpd2	3.28	3.27	Nucleic acid binding|mRNA processing factor
430836	2310047M15Rik	3.27	3.47	
900173	Ndufs6|LOC631040	3.26	3.06	Oxidoreductase
438004		3.26	3.10	
722262	Rps21	3.23	2.68	Nucleic acid binding|Ribosomal protein
752232	Cox8a	3.23	3.21	Oxidoreductase|Oxidase
761899	Lsm7	3.22	3.12	mRNA splicing factor|Nucleic acid binding|
887390	1700102H20Rik	3.22	4.07	mRNA processing factor
898883	LOC632624	3.22	4.22	Transcription factor
760128	Homer2	3.21	2.42	Signaling molecule|Other signaling molecule
917205	Ubl5	3.21	3.40	Molecular function unclassified
408125	Chchd7	3.21	3.44	Molecular function unclassified
893743	Rpl36	3.20	3.35	Ribosomal protein|Nucleic acid binding
898448	Hist2h2ac|Hist2h2ab	3.20	2.85	Histone|Nucleic acid binding
839914	2900010M23Rik	3.20	2.86	
773044	Ppp1r14a	3.20	2.38	Phosphatase inhibitor|Phosphatase modulator| Select regulatory molecule
896586	Cox7c	3.20	3.31	Oxidoreductase|Oxidase
832775	Ndufb4	3.18	3.16	Molecular function unclassified
543307	Ier3ip1	3.18	3.30	Molecular function unclassified
895475	LOC545790	3.18	3.45	Molecular function unclassified
912244	Ndufa5	3.17	3.18	Molecular function unclassified
307943		3.16	4.04	
930098	2010110K16Rik	3.15	3.11	
908623	Mrpl33	3.14	3.10	
895155	Hist1h2af	3.14	2.91	Histone|Nucleic acid binding
782574	Polr2i	3.14	3.02	Nucleotidyltransferase|Nucleic acid binding| DNA-directed RNA polymerase;Transferase
300922	Ndufa13	3.13	3.79	Molecular function unclassified
611934	Dbi	3.11	2.81	Other transfer/carrier protein; Select regulatory molecule| Transfer/carrier protein| Other enzyme regulator| Other enzyme inhibitor
899999	Magmas	3.11	2.80	Transporter| Other miscellaneous function protein| Other transporter; Miscellaneous function

895099	LOC636012|LOC621313|Snrpg|LOC432944	3.11	2.97	mRNA splicing factor|Nucleic acid binding|mRNA processing factor
893013	LOC223745	3.10	3.18	Nucleic acid binding|Ribosomal protein
777663	6330578E17Rik	3.10	2.25	
832518		3.09	3.12	
565544	Mrps21	3.09	3.12	Molecular function unclassified
587499	Timm10	3.07	2.55	Transfer/carrier protein|Mitochondrial carrier protein
893035	Hist1h2ak	3.07	2.86	Histone|Nucleic acid binding
923291	2310030G09Rik	3.06	2.32	Transcription factor|KRAB box transcription factor| Zinc finger transcription factor
341292	2410004N09Rik	3.06	3.29	
903480	Sec61g|LOC626569|LOC629406|LOC633091|LOC632898|LOC634859	3.06	3.30	Membrane traffic protein|Other membrane traffic protein
733908	2600009P04Rik	3.05	2.85	
741113	2810001A02Rik	3.05	2.83	
873382	1190007F08Rik	3.05	3.96	
868644	Polr2k	3.04	2.46	Molecular function unclassified
866075	Cnot4	3.03	2.55	Transcription factor;Nucleic acid binding
739525	Ndufb7	3.03	3.07	Molecular function unclassified
360511	Ndufb3	3.03	3.27	Molecular function unclassified
894817	Snrpe	3.02	3.11	mRNA splicing factor|Nucleic acid binding|mRNA processing factor
761984	1810008A14Rik	3.02	2.86	
462444	Atpif1	3.01	3.97	Miscellaneous function|Other miscellaneous function protein
799040	Cox6b1	3.01	2.89	Oxidoreductase|Oxidase
892069	1110017O22Rik	3.00	2.97	
517773	Mrp63	2.99	2.74	
390266	LOC623139|2510002D24Rik	2.99	2.71	
898986	LOC631712|Ndufs5|Ndufs5	2.98	3.03	Molecular function unclassified
481863	Cstb	2.97	2.81	Protease inhibitor|Cysteine protease inhibitor|Select regulatory molecule
461807	2310016E02Rik	2.97	2.60	
593829		2.97	3.22	
366364	Lsm7	2.96	3.04	mRNA splicing factor|Nucleic acid binding|mRNA processing factor
426384	LOC633788|D11Wsu99e|LOC544768	2.96	2.41	
900064		2.96	2.81	
805647	2010320M18Rik	2.96	2.85	
892462	LOC623970	2.96	2.98	Molecular function unclassified
494056	Hspe1	2.96	2.57	Chaperone|Chaperonin
451316	Hint2	2.95	2.97	Nucleotide phosphatase|Phosphatase
579357	LOC623465|Rnu17d	2.95	2.44	
439528	Srp19	2.93	2.96	Nucleic acid binding|Ribonucleoprotein;Membrane traffic protein| Membrane traffic regulatory protein
582022	Sp4	2.93	4.03	Transcription factor|Transcription cofactor;Nucleic acid binding| Zinc finger transcription factor| Other zinc finger transcription factor; Transcription factor|Other DNA-binding protein
778490	Ahi1	2.92	3.71	Molecular function unclassified
789613	Shfm1	2.92	2.95	Molecular function unclassified
916241	1500026D16Rik	2.91	2.70	Molecular function unclassified
926999	Ndufa6	2.91	2.83	Molecular function unclassified
930858	1110058L19Rik	2.91	2.69	
900234	Rpl36	2.90	2.99	Nucleic acid binding|Ribosomal protein
902439	LOC434460	2.90	2.84	Nucleic acid binding|Ribosomal protein
494868	Bsdc1	2.90	2.69	Molecular function unclassified

925617	Hoxc9	2.89	2.76	Transcription factor|Homeobox transcription factor;Nucleic acid binding| Other DNA-binding protein
353359	LOC435456	2.89	2.76	Oxidoreductase|Reductase
413747	Rtf1	2.88	2.82	Molecular function unclassified
896231	1100001I22Rik	2.87	3.05	Ribosomal protein|Nucleic acid binding
542048	Deb1	2.87	2.24	Nucleic acid binding|Chromatin/chromatin-binding protein
501866	2310003F16Rik	2.87	2.96	
898672	LOC435784	2.86	2.77	Ribosomal protein|Nucleic acid binding
893304	Gng5|LOC628007	2.85	2.76	Large G-protein|G-protein|Select regulatory molecule
879203	Ddx18|LOC545871| LOC627227| LOC640091	2.85	2.53	Helicase|Nucleic acid binding|RNA helicase
555617	AW049829	2.85	2.64	
908428	1810037I17Rik	2.85	3.32	
898865	Cox5b	2.85	2.67	Oxidoreductase|Oxidase
901532	LOC632013| LOC627746	2.84	2.89	Molecular function unclassified
427106	2410015N17Rik	2.84	2.63	
664157	Chchd5	2.84	2.12	Molecular function unclassified
494725	Hipk2	2.83	2.12	Non-receptor serine/threonine protein kinase|Protein kinase|Kinase
762026	LOC194197	2.83	2.96	Nucleic acid binding|Ribosomal protein
897505	LOC631000| LOC620313	2.83	2.97	Molecular function unclassified
818745	LOC384782	2.83	2.74	Ribosomal protein|Ribonucleoprotein;Nucleic acid binding| Nucleic acid binding
742821	1810030N24Rik	2.82	2.26	Molecular function unclassified
894875	Cox8a	2.82	2.87	Oxidoreductase|Oxidase
573930		2.82	2.53	
655753	Polr2j	2.81	2.51	Nucleotidyltransferase|Nucleic acid binding|DNA-directed RNA polymerase; Transferase
895153	Hist1h2an	2.81	2.50	Histone|Nucleic acid binding
681425	Stra13	2.81	3.24	
895528	Sec61g|LOC626569| LOC632898| LOC634859	2.80	2.96	Membrane traffic protein|Other membrane traffic protein
640297		2.80	2.49	Receptor|Other receptor;Cell adhesion molecule
607211	LOC212084	2.79	2.87	Nucleic acid binding|Ribosomal protein
589987	Atox1	2.79	2.73	
598135	2300009A05Rik	2.79	2.84	
467882	2210411K19Rik	2.78	2.23	
894895	1810022K09Rik	2.77	2.76	
600222	Uqcrq	2.77	2.31	Molecular function unclassified
893328		2.77	3.12	
347580	3110009E18Rik	2.76	2.84	
908871	Scand1	2.76	3.42	Transcription factor|Zinc finger transcription factor| Other zinc finger transcription factor
674723	Phlda1	2.76	2.45	Molecular function unclassified
457775	Grcc10	2.76	3.19	Molecular function unclassified
895740	Rps28	2.75	2.83	Nucleic acid binding|Ribosomal protein
773467	Emr1	2.74	2.77	Receptor|G-protein coupled receptor
658726	4930526I15Rik	2.74	2.47	
872246	AW209491	2.74	2.36	Molecular function unclassified
895170	Cdc2l1|Serf2	2.73	2.80	Non-receptor serine/threonine protein kinase|Protein kinase|Kinase| Molecular function unclassified
901543	Hist1h2ao	2.73	2.44	Histone|Nucleic acid binding
776936	Fau	2.73	2.62	Molecular function unclassified
903015	LOC634308| LOC619750	2.73	2.31	Cytokine|Signaling molecule
754818	Centb2	2.73	3.03	G-protein modulator|Nucleic acid binding;Select regulatory molecule| Other G-protein modulator

914192	Znhit1	2.72	2.37	Molecular function unclassified
650886	Mrpl34	2.72	2.46	
750696		2.71	2.56	
892288	LOC239245	2.71	2.68	Nucleic acid binding|Ribosomal protein
442460	1810008O21Rik	2.71	2.81	
919163	Fkbp2	2.71	2.62	Isomerase|Other isomerase
718537	Rps27l	2.70	2.57	Nucleic acid binding|Ribosomal protein
706194	Polr2f	2.69	2.52	DNA-directed RNA polymerase|Nucleic acid binding
658569	Crip1	2.69	3.97	Cytoskeletal protein|Actin binding cytoskeletal protein
412870	2410015M20Rik	2.69	2.54	
899117	LOC623265| LOC640777| LOC634885|Rps27	2.69	2.69	Ribosomal protein|Nucleic acid binding
927561	2810428I15Rik	2.68	2.76	
401451	Them2	2.68	2.23	Esterase|Hydrolase
659628	Ahi1	2.68	3.47	Molecular function unclassified
908701	S100a13	2.67	5.97	Calmodulin related protein|Select calcium binding protein
933097	Serf1	2.67	3.72	Molecular function unclassified
432753	2900006A08Rik	2.67	3.47	
901776	Mrpl23	2.67	2.69	Ribosomal protein|Nucleic acid binding
898302	Rpl38|LOC620192| LOC625646| LOC625492| LOC633352| LOC638514| LOC632400	2.66	2.73	Ribosomal protein|Nucleic acid binding
381804	1500012F01Rik	2.66	3.35	
897919		2.66	2.39	Nucleic acid binding|Ribosomal protein
898967	LOC623227| LOC433050	2.65	2.55	Nucleic acid binding|Ribosomal protein
343526	Mrpl54	2.65	3.11	
901822	LOC638943	2.65	2.87	Nucleic acid binding|Ribosomal protein
932283	2010204K13Rik	2.64	2.38	
893348		2.63	2.76	Molecular function unclassified
895273	LOC432822| LOC631451	2.63	2.93	Oxidoreductase|Reductase
699972	4930503B16Rik	2.63	3.13	Molecular function unclassified
899155	LOC629573| LOC635061	2.63	2.57	Nucleic acid binding|Ribosomal protein
734744	4930488E11Rik	2.62	3.22	Molecular function unclassified
735288	Nme4	2.62	2.14	Nucleotide kinase|Kinase
735363	1810017G16Rik	2.62	2.89	Molecular function unclassified
901911		2.62	2.87	
892363		2.62	2.68	
913372	Ccdc23	2.61	2.91	
866229	2400009B08Rik	2.61	2.85	
689028	Ndufb6	2.60	2.78	Molecular function unclassified
614321	Bat2d	2.59	2.06	Nuclease|Transcription factor;Nucleic acid binding
524776	Brd8	2.59	2.74	Molecular function unclassified
511364	2410006H16Rik	2.58	3.18	
901981	Psenen	2.58	2.28	Molecular function unclassified
614249	Higd2a	2.57	2.54	Molecular function unclassified
893620	Cox5b	2.56	2.72	Oxidoreductase|Oxidase
339156	Wbp4	2.56	2.51	Molecular function unclassified
350009	C330008K14Rik	2.55	2.24	Molecular function unclassified
430195	2900042B11Rik	2.55	2.88	
843424	Lig1	2.55	2.19	DNA ligase;Ligase|Nucleic acid binding|DNA ligase
432693	Zc3h6	2.54	2.53	Molecular function unclassified
574638	2600001A11Rik	2.54	2.39	
893675		2.54	2.55	
899691		2.53	2.50	

439122	AI413582	2.53	2.34	
715053	Mcee	2.53	2.18	Molecular function unclassified
463811	Tcfap2b	2.53	2.30	Other transcription factor|Transcription factor
646239	Mrpl14	2.52	2.56	Molecular function unclassified
522569	Rpl37a	2.52	2.27	Ribosomal protein|Nucleic acid binding
897920	Mrps16	2.52	2.40	Nucleic acid binding|Ribosomal protein
892769	Pdcd5	2.51	2.40	Select regulatory molecule
423067	2700070H01Rik	2.51	2.56	
895902	Sec61b	2.50	2.84	Molecular function unclassified
357529	D8Ertd738e	2.50	2.38	
659915	Mrps36| LOC633748	2.50	2.35	
620133	Lsm5|LOC546689	2.50	2.48	Molecular function unclassified
875883		2.50	4.35	
740898	BC051226	2.49	2.46	
832844	1300013D05Rik	2.49	2.35	Molecular function unclassified
896600	LOC623390| LOC627985| LOC631878| LOC631562| 0610038D11Rik	2.48	2.39	Molecular function unclassified
402550	Gstk1	2.48	3.05	Molecular function unclassified
408365	A030007L17Rik	2.47	2.86	Molecular function unclassified
900913	LOC631031| LOC627165| Lsm6|LOC635563	2.47	2.30	mRNA splicing factor|Nucleic acid binding|mRNA processing factor
396251	9430052C07Rik	2.47	2.98	
911759	Rpp21	2.47	2.32	Molecular function unclassified
755296	Anapc11	2.47	2.52	Transcription factor|Ubiquitin-protein ligase|Zinc finger transcription factor| Other zinc finger transcription factor; Ligase
674946	2700088M22Rik	2.47	2.30	Other RNA-binding protein| Nucleic acid binding
897828	2400002F11Rik	2.46	2.10	Other receptor| Receptor
932445	S100a6	2.46	3.57	Growth factor; Select calcium binding protein| Calmodulin related protein| Signaling molecule
566919	1100001I22Rik	2.46	2.21	Nucleic acid binding|Ribosomal protein
932445	S100a6	2.46	3.57	Growth factor;Select calcium binding protein|Calmodulin related protein| Signaling molecule
566919	1100001I22Rik	2.46	2.21	Nucleic acid binding|Ribosomal protein
895948	LOC632922| LOC628781| 1110017O22Rik| LOC628935	2.45	2.28	
923241	D11Bwg0434e	2.45	2.86	
551769	9130017A15Rik	2.45	2.65	Phosphatase|Protein phosphatase
907003	Vkorc1	2.44	2.39	Molecular function unclassified
741003	D2Bwg1335e	2.44	2.52	
924583	0610012D17Rik	2.44	2.60	Microtubule family cytoskeletal protein|Cytoskeletal protein
786436	Phpt1	2.44	2.61	Molecular function unclassified
897978	LOC635561| LOC622379	2.44	2.48	Molecular function unclassified
724513	Mrpl55	2.42	2.00	
922747	Zmat5	2.42	2.37	Nuclease|Nucleic acid binding
893226	LOC381346	2.42	2.48	
737829	LOC625603| LOC637655	2.41	2.62	Nucleic acid binding|Ribosomal protein
749867	LOC627737| LOC632026	2.41	2.45	Nucleic acid binding|Ribosomal protein
724898	Vamp2	2.41	2.29	SNARE protein|Membrane traffic protein
913188	0610039D01Rik	2.41	2.42	Transporter|Cation transporter
568926	5133401N09Rik	2.41	2.87	
892110	LOC621210	2.40	2.49	

333472	2810417J12Rik	2.40	2.21	
904383	LOC622873|LOC636663|Polr2k	2.40	2.41	Molecular function unclassified
627512	4632417K18Rik	2.40	2.34	
742847	LOC217600	2.40	2.36	Ribosomal protein|Nucleic acid binding
626399	Sema6a	2.40	2.30	Membrane-bound signaling molecule|Other signaling molecule; Signaling molecule|Signaling molecule
897153	Tbca	2.39	2.34	Molecular function unclassified
929926	Dtymk	2.38	2.25	Nucleotide kinase|Kinase
542023	1700021C14Rik	2.38	2.48	
904646	Snrpd1|LOC628807|LOC632595	2.38	2.54	Ribonucleoprotein| mRNA processing factor
685442		2.38	2.91	
765262	Zcsl2	2.37	2.48	Molecular function unclassified
927157	2010012C16Rik	2.37	1.88	Molecular function unclassified
537031	1110038B12Rik	2.37	2.49	
921470	Med31	2.37	2.41	Molecular function unclassified
925081	Chchd1	2.37	2.24	
637182	Rpo1-3	2.36	2.11	Nucleotidyltransferase|Nucleic acid binding|DNA-directed RNA polymerase; Transferase
416812	Nedd8	2.36	2.49	Nucleic acid binding|Ribosomal protein
920984	1110002E23Rik	2.36	2.01	
892426	LOC632599|Rpl37a	2.36	2.52	Nucleic acid binding|Ribosomal protein
926440	Gemin7	2.35	2.20	
739417	Mkks	2.35	2.12	Chaperone|Chaperonin
902785		2.34	2.36	
397332	Ddt	2.34	2.56	Isomerase
898453	Ndufc2	2.34	2.08	Oxidoreductase
346999	2310058O09Rik	2.33	3.20	
813192	2810432D09Rik	2.32	2.12	Molecular function unclassified
897331	Cks2|LOC626178|LOC635484|LOC633373	2.32	2.24	Molecular function unclassified
901658	LOC545028|LOC633871	2.32	2.30	Nucleic acid binding|Ribosomal protein
893574		2.32	2.35	Oxidoreductase|Reductase
886579	Cdkn3	2.31	2.04	Phosphatase|Protein phosphatase
745538	2610510H03Rik	2.31	2.75	
927369	1500032L24Rik	2.31	2.58	
897385	Atp5g1	2.31	2.12	Transporter|Cation transporter|ATP synthase|Synthase|Hydrogen transporter; Synthase and synthetase
563929		2.31	2.22	
893075	Hist1h2an|Hist1h2ai|Hist2h3c1|Hist1h2ac|Hist2h2ab|Hist1h2ah|Hist1h2ae|H2afx|Hist2h2aa2|Hist2h2aa1|Hist1h2ad|Hist1h2ag|Hist1h2ao|Hist2h2ac|Hist1h2af|Hist1h2ab	2.31	1.95	Histone|Nucleic acid binding
644189	1810058I14Rik	2.31	2.40	
901018	LOC622236|LOC639189	2.30	2.25	Nucleic acid binding|Ribosomal protein
710865	LOC640072	2.30	2.24	
896694	Carhsp1	2.30	2.18	Other RNA-binding protein|Nucleic acid binding
604576	LOC383438	2.30	2.77	Nucleic acid binding|Ribosomal protein

900726	Atp5j	2.30	2.08	Transporter|Synthase|Cation transporter|Hydrogen transporter; Synthase and synthetase
453514	3110023B02Rik	2.30	2.11	Molecular function unclassified
397058		2.29	2.36	
899772	Supt4h2	2.29	2.40	Transcription factor|Chromatin/chromatin-binding protein| Basal transcription factor; Nucleic acid binding
930166	D530033C11Rik	2.29	1.98	Molecular function unclassified
806366	2210015D19Rik	2.28	2.23	Ligase| Other ligase
362443	Pscd1	2.28	2.81	G-protein modulator| Guanyl-nucleotide exchange factor| Select regulatory molecule
900918	Rpl36a	2.28	2.41	Molecular function unclassified
906238	S100a4	2.28	3.57	Calmodulin related protein| Select calcium binding protein
655384	1810014F10Rik	2.27	1.91	
580691	Lsm3	2.27	1.98	mRNA splicing factor| Nucleic acid binding|mRNA processing factor
920448	Pop5	2.27	2.16	Molecular function unclassified
895199	LOC627075| LOC633571	2.27	2.26	Nucleic acid binding| Ribosomal protein
531323	C430049B03Rik	2.26	2.56	
784425	2310040G24Rik	2.26	2.30	
897733	LOC622384| LOC634810	2.26	2.29	Other transfer/carrier protein| Transfer/carrier protein
643466	C730025P13Rik	2.26	1.89	
750862	Ropn1l	2.25	1.90	
892057		2.25	1.94	
470448	LOC383436	2.25	2.18	Nucleic acid binding| Ribosomal protein
729481	Pfdn5	2.25	2.43	Chaperone
892317	LOC546052	2.25	2.17	Ribosomal protein| Nucleic acid binding
409582	Pfdn1	2.24	2.21	Molecular function unclassified
906456	Ndufa12	2.24	2.12	Oxidoreductase
406680	Hes1	2.24	2.30	Transcription factor| Basic helix-loop-helix transcription factor; Nucleic acid binding
510011	2410003K15Rik	2.24	2.06	
757052	LOC635189|Nenf| LOC635176	2.23	2.69	Signaling molecule
896346	Edf1	2.23	2.40	Transcription factor| Transcription cofactor;Nucleic acid binding
362464	Ubl4	2.23	1.85	Ribosomal protein| Nucleic acid binding
895541	LOC637250| LOC625917	2.23	2.20	Nucleic acid binding| Ribosomal protein
547326	2310010J17Rik	2.23	3.00	
433736	0610012G03Rik	2.22	2.32	
325139		2.22	2.13	
381544	Rpia	2.22	2.11	Isomerase| Epimerase/ racemase
899360	LOC622978| LOC631214	2.21	2.05	Ribosomal protein| Nucleic acid binding
920354	Magoh	2.21	1.91	Molecular function unclassified
894311	LOC432535| LOC634567| LOC623483	2.21	2.26	Ribosomal protein| Nucleic acid binding
351750	Phf23	2.20	2.18	Molecular function unclassified
901877	Rpl39	2.20	2.54	Nucleic acid binding| Ribosomal protein
894561		2.19	2.30	
901421	LOC637993	2.19	2.28	Nucleic acid binding| Ribosomal protein
891902	2610034E18Rik	2.19	2.01	
759997	LOC546740| LOC631915	2.19	2.02	Nucleic acid binding| Ribosomal protein
487148	3110003A17Rik	2.18	2.01	
548465	Rps24	2.18	2.03	Nucleic acid binding| Ribosomal protein
892212	Rps15a|LOC435784	2.18	2.33	Ribosomal protein| Nucleic acid binding
336338	Lix1	2.17	2.19	
517258	LOC382340	2.17	2.24	Ribosomal protein| Nucleic acid binding
634492	LOC630651| LOC623177	2.17	2.14	Ribosomal protein|Nucleic acid binding

900297	LOC626920|LOC640355|Brp17	2.16	2.20	Other hydrolase|Hydrolase
626108	Chd4	2.16	1.97	DNA helicase|Helicase|Nucleic acid binding
896788	LOC631649	2.16	2.22	Nucleic acid binding|Ribosomal protein
508952	1700013G20Rik	2.16	2.09	Molecular function unclassified
792591	A330050F15Rik	2.16	2.14	
737177	1110019J04Rik	2.16	1.96	
896827	Mrps33	2.15	2.48	Nucleic acid binding|Ribosomal protein
581260	M6prbp1	2.15	2.26	Transfer/carrier protein
484120	Rpl28	2.15	2.19	Ribosomal protein|Nucleic acid binding
901896	LOC631287	2.15	2.46	Miscellaneous function|Other miscellaneous function protein
706669	1500032D16Rik	2.15	2.54	Molecular function unclassified
369399	0610010K14Rik	2.15	2.34	Nucleic acid binding
900666	Rps8	2.15	2.18	Ribosomal protein|Nucleic acid binding
430527	LOC434860	2.15	2.29	Chaperone
646887	5430405G24Rik	2.14	1.92	Molecular function unclassified
577127	LOC621892|Atp5j|LOC640508	2.14	2.02	Transporter| Synthase| Cation transporter| Hydrogen transporter; Synthase and synthetase
688390	2700094K13Rik	2.14	1.96	
904285	Rbx1	2.14	2.38	Transcription factor|Ubiquitin-protein ligase|Zinc finger transcription factor| Other zinc finger transcription factor; Ligase
631849	Ppp1r11	2.14	1.97	Molecular function unclassified
719899	4930535B03Rik	2.13	1.97	Molecular function unclassified
314402	1200016B10Rik	2.13	1.89	Molecular function unclassified
901878	LOC629695|LOC637673	2.13	2.39	Nucleic acid binding|Ribosomal protein
914463	1110008P14Rik	2.13	2.36	
916326	Taf9	2.12	2.10	Transcription factor|Basal transcription factor;Nucleic acid binding
899617	LOC632311|LOC625038	2.12	2.16	Nucleic acid binding|Ribosomal protein
891768	Rpl36a	2.12	2.13	Molecular function unclassified
686285	Mrpl18	2.11	1.97	Molecular function unclassified
905986	Mrps28	2.11	2.27	Nuclease|Nucleic acid binding
329437	Itgb3bp	2.11	2.00	
811604	2410085M17Rik	2.11	2.47	
807241	Dnajc4	2.11	2.11	Chaperone|Other chaperones
896593	LOC623568|LOC635255	2.11	2.39	Nucleic acid binding|Ribosomal protein
755608	1700026B20Rik	2.10	2.38	
797634	AI462493	2.10	2.03	
900821		2.10	2.00	Ribosomal protein|Nucleic acid binding
916253	Sepw1	2.10	2.28	Molecular function unclassified
907754	Drap1	2.09	2.12	Other transcription factor|Transcription factor
905629	2010316F05Rik	2.09	1.86	
895303	Ndufab1	2.09	2.38	Transfer/carrier protein
309143	Rpl36al	2.09	2.35	Molecular function unclassified
606418	Nrxn1	2.09	2.07	Other receptor|Receptor
933122	Clpb|LOC639045|LOC634909|Rpl31|LOC635626|LOC638399	2.09	2.05	Nucleic acid binding|Ribosomal protein|Hydrolase
901949	6330405D24Rik|LOC625403	2.09	2.27	Other transfer/carrier protein|Transfer/carrier protein
892561	LOC635276|LOC385412	2.09	2.29	Molecular function unclassified
376116	Centg1	2.09	2.66	G-protein modulator|Nucleic acid binding;Select regulatory molecule| Other G-protein modulator
892595	Uqcrb	2.08	2.24	Oxidoreductase|Reductase
677926	1190005I06Rik	2.08	2.57	
334855	Hist1h2bm	2.08	2.48	Molecular function unclassified
368174	Gchfr	2.07	2.70	

908398	Efcab2	2.07	1.99	Molecular function unclassified
469209	Cd302	2.07	1.82	
472385	H2afv	2.07	2.68	Histone|Nucleic acid binding
747743	Crabp1	2.07	2.48	Other transfer/carrier protein|Transfer/carrier protein
686407	Nrxn2	2.07	1.84	Other receptor|Receptor
894223	Cox7b|LOC625784	2.07	2.04	Molecular function unclassified
803435	1110019N10Rik	2.07	1.94	Molecular function unclassified
902449	LOC433387| LOC633404	2.06	2.52	Ribosomal protein|Nucleic acid binding
896315	Rbx1	2.05	2.16	Transcription factor|Ubiquitin-protein ligase|Zinc finger transcription factor| Other zinc finger transcription factor;Ligase
895011	LOC194960| LOC630041	2.05	2.02	Nucleic acid binding|Ribosomal protein
644434	D11Ertd99e	2.04	2.18	
901081	LOC632169| LOC624713	2.04	2.15	Molecular function unclassified
929017	Pcdha11|Pcdha7| Pcdha6|Pcdha1| Pcdha8|Pcdhac2| Pcdha9|Pcdhac1| Pcdha3|Pcdha4| Pcdha2|Pcdha10| Pcdha5|Pcdha12	2.03	2.57	Cell adhesion molecule| Cadherin
910715	Sepm	2.03	2.24	
424741	LOC622881	2.03	1.95	Basal transcription factor| Transcription factor
909249	5830445C04Rik	2.03	2.07	Methyltransferase| Transferase
394580	3300001G02Rik	2.03	1.82	
359400	Timm17b	2.03	2.27	Transfer/carrier protein| Mitochondrial carrier protein
572587	LOC629300	2.01	1.88	
914553	Zranb1	2.01	1.79	Molecular function unclassified
321757	2810403D21Rik	2.00	2.37	
381433	Mettl1	2.00	1.94	Methyltransferase|Transferase
864277	Mrpl18	2.00	1.84	Molecular function unclassified
763666	Ndufs4	2.00	1.98	Molecular function unclassified
926911	Plekhj1	1.99	2.00	G-protein modulator|Guanyl-nucleotide exchange factor| Select regulatory molecule
928491	Pex19	1.99	2.33	Storage protein|Miscellaneous function
372374	2610208E05Rik	1.99	2.25	Molecular function unclassified
424621	Tsc22d1	1.99	2.30	Other transcription factor|Transcription factor
928949	Dynlrb1	1.99	2.25	Microtubule family cytoskeletal protein|Cytoskeletal protein
457831	2310056P07Rik	1.99	2.36	Molecular function unclassified
666974	Hcfc1r1	1.98	2.78	
916978	2210408F21Rik	1.98	2.32	
900524	Immp1l|LOC433890	1.98	2.07	Serine protease|Protease
501879	Mrpl53	1.97	2.15	
547782	LOC638884|Rwdd1| LOC545442	1.97	1.89	Molecular function unclassified
866961	2900009C16Rik	1.97	2.59	
631704	Coq7	1.97	2.00	Oxidoreductase|Oxygenase
617638	Nova1|G630039L02	1.97	1.91	mRNA splicing factor|Nucleic acid binding|mRNA processing factor
590982	Rpl22l1	1.97	1.85	Nucleic acid binding|Ribosomal protein
624658	4921506J03Rik	1.96	2.05	
334822	Sfxn1	1.96	2.16	Transporter|Other transfer/carrier protein|Cation transporter; Transfer/carrier protein
469731	Mrpl21	1.95	1.81	Molecular function unclassified
846124	Gngt2	1.95	2.28	Large G-protein|G-protein|Select regulatory molecule

932500	2810410M20Rik	1.95	1.96	Molecular function unclassified
422587	Eppb9	1.94	2.12	Molecular function unclassified
570781	5730509C05Rik	1.94	2.43	Molecular function unclassified
462543	LOC628595| LOC631796	1.94	2.05	Transcription factor|KRAB box transcription factor| Zinc finger transcription factor
434863	Cyb5	1.92	1.95	Oxidoreductase|Oxidase
926434	Mylpf	1.92	1.99	Other actin family cytoskeletal protein;Select calcium binding protein| Calmodulin related protein| Cytoskeletal protein| Actin binding cytoskeletal protein
898267	LOC638943| C330007P06Rik|Rpl39| LOC629695| LOC629229| LOC637673	1.91	2.06	Nucleic acid binding|Ribosomal protein|Molecular function unclassified
894728	LOC270040| LOC619780	1.91	2.03	Other transfer/carrier protein|Transfer/carrier protein
900393		1.91	1.80	
431274	Hint1	1.90	1.95	Nucleotide phosphatase|Phosphatase
916473	Ift20	1.90	2.17	
657074	Trappc1	1.90	1.92	Membrane traffic protein|Other membrane traffic protein
895424	LOC383341	1.90	2.02	Nucleic acid binding|Ribosomal protein
909084	1810046J19Rik	1.89	2.05	Molecular function unclassified
904296	LOC240853	1.89	1.98	Molecular function unclassified
436091	2410016F19Rik	1.89	1.96	Molecular function unclassified
541892		1.89	2.31	
897399	Rps15	1.88	1.92	Nucleic acid binding|Ribosomal protein
915242	Commd6	1.88	2.20	
654112	1110004B13Rik	1.87	2.03	
872960	2900011O08Rik	1.87	2.02	Molecular function unclassified
908496	Npy	1.86	2.75	Peptide hormone|Neuropeptide|Signaling molecule
732409	Rab33a	1.86	2.01	Small GTPase|G-protein|Select regulatory molecule
923547	Esrra	1.86	1.86	Molecular function unclassified
897017	Ifitm2	1.86	2.37	Miscellaneous function|Other miscellaneous function protein
361527	1810013D10Rik	1.85	1.88	
893211	LOC628298| LOC637129	1.85	1.93	Other transfer/carrier protein|Transfer/carrier protein
897860		1.85	1.95	
894331	LOC546246	1.85	1.94	Nucleic acid binding|Ribosomal protein
498966	Mthfs	1.85	2.10	Ligase|Other ligase
467529	Hmgn3	1.85	1.93	Nucleic acid binding|Chromatin/chromatin-binding protein
902457	LOC628061| LOC633920|Rps13 |LOC637251| LOC625298	1.84	1.84	Molecular function unclassified
930156	1810059G22Rik	1.84	1.85	
618976	Fkbp7	1.83	1.92	Other chaperones; Isomerase| Chaperone| Other isomerase
900296	LOC623114| LOC639478	1.82	1.92	Nucleic acid binding|Ribosomal protein
892239	LOC633908|Rps19| LOC269365| LOC627475| LOC639374| LOC625929	1.82	1.78	Nucleic acid binding|Ribosomal protein
906417	Synj2bp| 1810020G14Rik	1.82	2.03	Miscellaneous function|Other miscellaneous function protein
650447	Xpa	1.81	1.87	Damaged DNA-binding protein|Nucleic acid binding
898243	LOC625281| LOC633843	1.81	1.82	Nucleic acid binding|Ribosomal protein

365414	Tspan8	1.79	2.03	Other cell adhesion molecule|Membrane-bound signaling molecule; Cell adhesion molecule| Signaling molecule
832595	Agl	1.79	2.08	Molecular function unclassified
898192	LOC639196|Ero1l| Rpl31|LOC638399| LOC631731| LOC544868| LOC632618	1.79	1.79	Oxidoreductase|Ribosomal protein|Other oxidoreductase|Nucleic acid binding
891692	LOC640734	1.79	1.98	Ribosomal protein|Nucleic acid binding
903111	LOC626175|Rps26| LOC633195	1.79	1.93	Nucleic acid binding|Ribosomal protein
498407	Tmem50a	1.78	1.81	Molecular function unclassified
793761	Rpl14	1.78	1.81	Ribosomal protein|Nucleic acid binding
409810	Dpm2	1.78	1.90	
365301	Anapc10	1.77	1.75	Select regulatory molecule;Ligase|Other ligase
395784	Srp14	1.77	1.84	Other RNA-binding protein|Nucleic acid binding
898495	Atp5h	1.77	1.74	Molecular function unclassified
907987	Acyp1	1.76	2.32	Other phosphatase|Phosphatase
891680	LOC432725| LOC631612	1.75	1.89	Nucleic acid binding|Ribosomal protein
576893	Tmem42	1.74	2.02	
533074	Acyp2	1.74	2.47	Other phosphatase|Phosphatase
735094		1.73	1.78	
931922	0610010K14Rik	1.73	1.98	Nucleic acid binding
684608	Rala	1.73	1.92	Small GTPase|G-protein|Select regulatory molecule
626898	Tmem60	1.69	1.83	
899662	LOC545783| LOC632337|Odc1	0.61	0.51	Molecular function unclassified
692827	Rad23b	0.59	0.42	Nucleic acid binding|Damaged DNA-binding protein
667619	Kars|LOC631033	0.59	0.56	Nucleic acid binding|Synthetase|Aminoacyl-tRNA synthetase| Other RNA-binding protein; Synthase and synthetase
903368	Ldha	0.59	0.50	Oxidoreductase|Dehydrogenase
906972	4930503L19Rik	0.59	0.54	
748512	Tars	0.58	0.45	Other ligase|Synthetase;Ligase|Synthase and synthetase
338639	Immt	0.58	0.58	Molecular function unclassified
406056	Ube1c	0.58	0.55	Ligase|Other ligase
893225	Tcea1	0.58	0.50	Transcription factor|Basal transcription factor;Nucleic acid binding
905037	Pnpt1	0.57	0.56	Nuclease|Exoribonuclease;Transferase|Esterase|Nucleic acid binding| Nucleotidyltransferase; Hydrolase
902369	Hspd1	0.57	0.42	Chaperone|Chaperonin
532062	Skiv2l2	0.57	0.51	Helicase|Nucleic acid binding|DNA helicase;Hydrolase
880005	5730445M16Rik	0.57	0.44	Molecular function unclassified
850262	Rbbp4	0.57	0.54	Miscellaneous function|Other miscellaneous function protein
896848	Eef1g	0.56	0.55	Nucleic acid binding|Translation factor|Other cytoskeletal proteins|
900427		0.56	0.50	
844889	Ogt	0.56	0.55	Glycosyltransferase|Transferase
895480	LOC383528| LOC433326| LOC433923| LOC630624|Slc25a5	0.56	0.48	Transporter;Transfer/carrier protein|Mitochondrial carrier protein
913622	Atp5b	0.55	0.51	Synthase|Cation transporter|ATP synthase;Hydrolase|Ion channel| Hydrogen transporter;Synthase and synthetase|Other ion channel;Transporter

759487	Nxt2	0.55	0.40	Miscellaneous function|Other miscellaneous function protein
467179	Cct6a	0.55	0.48	Chaperone|Chaperonin
321598	Tagln2	0.55	0.54	Cytoskeletal protein|Non-motor actin binding protein| Actin binding cytoskeletal protein
551673	Eif4g2	0.55	0.33	Translation initiation factor|Nucleic acid binding|Translation factor
914228	Vim	0.54	0.52	Structural protein|Cytoskeletal protein|Intermediate filament; Miscellaneous function
929416	Cct2	0.54	0.47	Chaperone|Chaperonin
752329	Nap1l1	0.54	0.53	Phosphatase inhibitor|Phosphatase modulator|Select regulatory molecule
468332	Hnrpab	0.54	0.50	Nucleic acid binding|Ribonucleoprotein
897674	Ldha	0.53	0.47	Oxidoreductase|Dehydrogenase
742632	Cct4	0.53	0.49	Chaperone|Chaperonin
327644	LOC636981	0.53	0.50	
379659	LOC633677|Eprs	0.52	0.43	DNA ligase;Ligase|Nucleic acid binding|Other ligase
900759	LOC628388| LOC634513 LOC547402| LOC545545| LOC545864| LOC545543| LOC630487|Rpl3| LOC242809|	0.52	0.51	Nucleic acid binding|Ribosomal protein|Molecular function unclassified
755334	Hdac9	0.52	0.50	Deacetylase|Nucleic acid binding;Hydrolase
537344	Cct8	0.52	0.45	Chaperone|Chaperonin
840369	Mgat2	0.52	0.56	Glycosyltransferase|Transferase
904921	Rnf187	0.52	0.45	Ligase|Ubiquitin-protein ligase
510362	Atad2	0.52	0.49	Molecular function unclassified
422109	Tcp1	0.51	0.47	Chaperone|Chaperonin
897885	Dstn	0.51	0.53	Cytoskeletal protein|Non-motor actin binding protein| Actin binding cytoskeletal protein
494196	Dcamkl1	0.51	0.50	Non-receptor serine/threonine protein kinase|Protein kinase| Non-motor microtubule binding protein; Kinase| Microtubule family cytoskeletal protein| Cytoskeletal protein
910111	Asns	0.51	0.43	Other ligase|Synthetase;Ligase|Synthase and synthetase
916212	Ywhae	0.51	0.56	Molecular function unclassified
894795		0.51	0.50	
613107	LOC634398| LOC624287|Hnrpk| LOC636506| LOC544961	0.51	0.53	Nucleic acid binding|Ribonucleoprotein
813812	Nucks1	0.51	0.48	Molecular function unclassified
902940	LOC544863| LOC638893	0.51	0.51	Microtubule family cytoskeletal protein|Tubulin|Cytoskeletal protein
911591	Sfrs2	0.51	0.50	mRNA splicing factor|Nucleic acid binding|mRNA processing factor
768588	LOC432633| Pgk1|LOC433594	0.51	0.42	Kinase|Carbohydrate kinase
922635	Vdac1	0.50	0.45	Voltage-gated ion channel|Ion channel|Anion channel;Ion channel
900946	Kpna2	0.50	0.42	Transfer/carrier protein
902405	LOC624793|Mfap1	0.50	0.50	Other extracellular matrix|Extracellular matrix
907265	Hnrpu	0.50	0.46	Other RNA-binding protein|Nucleic acid binding
455377	Cct7	0.50	0.49	Chaperone|Chaperonin
858702	Ddx3x	0.50	0.48	Helicase|Nucleic acid binding|RNA helicase
551559	H1f0	0.50	0.53	Histone|Nucleic acid binding
921273	Atp5a1	0.50	0.47	Molecular function unclassified

845286	Gars	0.50	0.38	Aminoacyl-tRNA synthetase;Ligase|Synthase and synthetase|Synthetase
360356	Rtn4	0.49	0.50	Signaling molecule|Other signaling molecule
901275	LOC628192	0.49	0.45	Cytoskeletal protein|Actin and actin related protein| Actin binding cytoskeletal protein
725830	Hnrph1	0.49	0.51	Nucleic acid binding|Ribosomal protein
552143	Cct3	0.49	0.49	Chaperone|Chaperonin
566593	Hsd17b12	0.49	0.53	Oxidoreductase|Dehydrogenase;Oxidoreductase|Reductase
797894	Lgmn	0.49	0.57	Cysteine protease|Protease
893894	Psat1	0.49	0.40	Transferase|Transaminase
371253	Lamp1	0.48	0.50	Other miscellaneous function protein;Membrane traffic protein|
922881	Wbscr1	0.48	0.50	Translation initiation factor|Nucleic acid binding|Translation factor
895336		0.48	0.52	
904995	Ddx5	0.48	0.47	Helicase|Nucleic acid binding|RNA helicase
903400	LOC629372| LOC620390| LOC625467| LOC634792| LOC623634| LOC213079| LOC640060| LOC546331| LOC434174| Hmgb1| LOC385454| LOC632447	0.47	0.58	Molecular function unclassified
856479	Rsl1d1	0.47	0.38	Ribosomal protein|Nucleic acid binding
731074	Nsun2	0.47	0.50	Nucleic acid binding;Transferase|Methyltransferase
902241	Hspd1|Hspd1	0.47	0.40	Chaperone|Chaperonin
898562	LOC625349| LOC545942	0.46	0.37	Phosphatase inhibitor|Phosphatase modulator|Select regulatory molecule
898366	Actg1	0.46	0.36	Cytoskeletal protein|Actin and actin related protein| Actin binding cytoskeletal protein
841551	Arfip1	0.46	0.51	G-protein modulator|Other G-protein modulator|Select regulatory molecule
923112	Cnbp1	0.46	0.45	Nucleic acid binding
915817	Emp1	0.46	0.55	Other cytoskeletal proteins|Cytoskeletal protein
666306	LOC433225	0.45	0.42	Helicase|Nucleic acid binding|RNA helicase
902908	Eef2	0.45	0.55	Translation elongation factor|Nucleic acid binding|Translation factor
903688	Eif4a1	0.45	0.41	Helicase|Nucleic acid binding|RNA helicase
888679	Kbtbd11|LOC632344	0.45	0.52	Molecular function unclassified
366579	LOC629758	0.45	0.48	Hsp 90 family chaperone|Chaperone
396629		0.45	0.40	
495530	LOC628890| LOC546148|Cd209c| LOC433000| LOC433002	0.44	0.41	Receptor| Other receptor; Cell adhesion molecule| Other defense and immunity protein| Other cell adhesion molecule; Defense/immunity protein| Molecular function unclassified
897529	Nono| LOC434808| LOC636259	0.44	0.42	mRNA splicing factor|Nucleic acid binding|mRNA processing factor
339036	Prph1	0.44	0.42	Structural protein| Cytoskeletal protein| Intermediate filament; Miscellaneous function
390796	Slc16a1	0.43	0.46	Transporter|Other transporter
468172	Hdac10	0.42	0.56	Deacetylase|Nucleic acid binding;Hydrolase

473515	Ppp2ca	0.41	0.38	Molecular function unclassified
906008	Serinc1	0.40	0.49	Transmembrane receptor regulatory/adaptor protein|Miscellaneous function
907017	Ncl	0.40	0.35	Other RNA-binding protein| Nucleic acid binding
302796	LOC280487|Sgip1	0.37	0.30	
920252	Mest	0.37	0.35	Serine protease|Protease
873436	Tubb5	0.36	0.50	Microtubule family cytoskeletal protein|Tubulin|Cytoskeletal protein
895685	Ywhaz	0.36	0.40	Molecular function unclassified
371118	Mtap1b	0.35	0.42	Non-motor microtubule binding protein| Microtubule family cytoskeletal protein| Cytoskeletal protein
803617	St18	0.35	0.54	Transcription factor|Zinc finger transcription factor| Other zinc finger transcription factor
458210	Kbtbd2| Ppp1r7| Def6|	0.33	0.38	
857880	4930556P03Rik| Akap8| D230044P21Rik| 1300012G16Rik| Aqp7| Gnl3l| Birc5| Supt6h| D4Ertd429e| 1110067I12Rik	0.33	0.35	Transcription factor|Transporter|Protease inhibitor|Other signaling molecule; Select regulatory molecule| G-protein;Hydrolase|Chromatin/chromatin-binding; protein| Other transporter| Miscellaneous function| Other miscellaneous function; protein|Signaling molecule|Phosphatase modulator|Basal transcription factor; Nucleic acid binding|Select regulatory molecule|Molecular function unclassified
770220	Rgs5	0.25	1.74	G-protein modulator|Other G-protein modulator|Select regulatory molecule
830062	Dennd2d	0.18	0.20	Molecular function unclassified
332421		0.12	0.16	

Supplementary Table S5A - Differently expressed gene ontology (GO) groups. Cellular components in negative control versus siDCL-2 comparison. Only GO classes and parent classes with at least 5 observations in the selected subset and with an 'Observed vs. Expected' ratio of at least 2 are shown.

GO id	GO classification	Observed in selected subset	Expected in selected subset	Observed/ Expected
5732	small nucleolar ribonucleoprotein complex	6.00	1.00	5.97
16469	proton-transporting two-sector ATPase complex	7.00	1.34	5.23
5830	cytosolic ribosome (sensu Eukaryota)	7.00	1.41	4.98
786	nucleosome	6.00	1.21	4.98
5746	mitochondrial electron transport chain	6.00	1.27	4.72
44455	mitochondrial membrane part	9.00	1.94	4.63
44452	nucleolar part	9.00	1.94	4.63
15935	small ribosomal subunit	6.00	1.34	4.48
5840	ribosome	28.00	6.83	4.10
19866	organelle inner membrane	25.00	6.29	3.97
5740	mitochondrial envelope	20.00	5.69	3.51
16591	DNA-directed RNA polymerase II\, holoenzyme	5.00	1.47	3.39
5743	mitochondrial inner membrane	15.00	4.49	3.34
44429	mitochondrial part	27.00	8.44	3.20
44445	cytosolic part	8.00	2.54	3.14
31966	mitochondrial membrane	15.00	4.82	3.11
5761	mitochondrial ribosome	7.00	2.28	3.07
313	organellar ribosome	7.00	2.28	3.07
31975	envelope	31.00	10.38	2.99
31967	organelle envelope	30.00	10.11	2.97
30529	ribonucleoprotein complex	43.00	14.46	2.97
5834	heterotrimeric G-protein complex	5.00	1.81	2.77
5730	nucleolus	11.00	4.35	2.53
31980	mitochondrial lumen	7.00	2.88	2.43
5759	mitochondrial matrix	7.00	2.88	2.43
19897	extrinsic to plasma membrane	5.00	2.08	2.41
5739	mitochondrion	78.00	33.28	2.34
785	chromatin	8.00	3.48	2.30
31090	organelle membrane	34.00	15.33	2.22
19898	extrinsic to membrane	5.00	2.28	2.20

Supplementary Table S5B - Differently expressed gene ontology (GO) groups. Cellular components in negative control versus siDCL-3 comparison. Only GO classes and parent classes with at least 5 observations in the selected subset and with an 'Observed vs. Expected' ratio of at least 2 are shown.

GO id	GO classification	Observed in selected subset	Expected in selected subset	Observed/ Expected
786	nucleosome	8.00	1.06	7.52
5830	cytosolic ribosome (sensu Eukaryota)	7.00	1.24	5.64
5746	mitochondrial electron transport chain	6.00	1.12	5.34
44455	mitochondrial membrane part	9.00	1.71	5.25
16469	proton-transporting two-sector ATPase complex	6.00	1.18	5.07
44452	nucleolar part	7.00	1.71	4.08
44445	cytosolic part	9.00	2.25	4.01
19866	organelle inner membrane	22.00	5.56	3.96
5840	ribosome	23.00	6.03	3.81
5743	mitochondrial inner membrane	14.00	3.96	3.53
5740	mitochondrial envelope	17.00	5.03	3.38
31966	mitochondrial membrane	14.00	4.26	3.29
785	chromatin	9.00	3.07	2.93
30529	ribonucleoprotein complex	37.00	12.77	2.90
31975	envelope	26.00	9.16	2.84
44429	mitochondrial part	21.00	7.45	2.82
31967	organelle envelope	25.00	8.93	2.80
5730	nucleolus	9.00	3.84	2.34
5739	mitochondrion	66.00	29.38	2.25
31090	organelle membrane	30.00	13.54	2.22

Supplementary Table S5C - Differently expressed gene ontology (GO) groups. Biologic processes in negative control versus siDCL-2 comparison. Only GO classes and parent classes with at least 5 observations in the selected subset and with an 'Observed vs. Expected' ratio of at least 2 are shown.

GO id	GO classification	Observed in selected subset	Expected in selected subset	Observed/ Expected
15986	ATP synthesis coupled proton transport	7.00	1.16	6.02
15985	energy coupled proton transport\, down electrochemical gradient	7.00	1.16	6.02
6119	oxidative phosphorylation	10.00	1.77	5.63
9142	nucleoside triphosphate biosynthetic process	9.00	1.65	5.45
6754	ATP biosynthetic process	7.00	1.29	5.45
6753	nucleoside phosphate metabolic process	7.00	1.29	5.45
9206	purine ribonucleoside triphosphate biosynthetic process	8.00	1.53	5.23
9201	ribonucleoside triphosphate biosynthetic process	8.00	1.53	5.23
9145	purine nucleoside triphosphate biosynthetic process	8.00	1.53	5.23
46034	ATP metabolic process	7.00	1.41	4.97
9205	purine ribonucleoside triphosphate metabolic process	8.00	1.65	4.84
9199	ribonucleoside triphosphate metabolic process	8.00	1.65	4.84
9141	nucleoside triphosphate metabolic process	9.00	1.90	4.74
9144	purine nucleoside triphosphate metabolic process	8.00	1.71	4.67
15992	proton transport	7.00	1.59	4.40
9152	purine ribonucleotide biosynthetic process	8.00	1.96	4.09
9260	ribonucleotide biosynthetic process	8.00	2.08	3.84
6818	hydrogen transport	7.00	1.84	3.81
6752	group transfer coenzyme metabolic process	7.00	1.90	3.69
1505	regulation of neurotransmitter levels	5.00	1.41	3.55
9150	purine ribonucleotide metabolic process	8.00	2.33	3.44
6164	purine nucleotide biosynthetic process	8.00	2.33	3.44
7046	ribosome biogenesis and assembly	8.00	2.39	3.35

GO id	GO classification	Observed in selected subset	Expected in selected subset	Observed/ Expected
9108	coenzyme biosynthetic process	9.00	2.69	3.34
30003	cation homeostasis	5.00	1.53	3.27
6875	metal ion homeostasis	5.00	1.53	3.27
9259	ribonucleotide metabolic process	8.00	2.51	3.19
6873	cell ion homeostasis	5.00	1.65	3.03
6457	protein folding	20.00	6.67	3.00
6163	purine nucleotide metabolic process	8.00	2.81	2.84
51188	Cofactor biosynthetic process	9.00	3.24	2.77
50801	ion homeostasis	5.00	1.84	2.72
6118	Electron transport	22.00	8.26	2.66
48878	chemical homeostasis	5.00	2.02	2.48
6412	translation	30.00	12.42	2.41
9165	nucleotide biosynthetic process	9.00	3.79	2.37
19725	cell homeostasis	5.00	2.20	2.27
15672	monovalent inorganic cation transport	10.00	4.41	2.27
6732	coenzyme metabolic process	12.00	5.39	2.23
65004	protein-DNA complex assembly	5.00	2.26	2.21
6091	generation of precursor metabolites and energy	33.00	14.93	2.21
22613	ribonucleoprotein complex biogenesis and assembly	13.00	6.18	2.10
7268	Synaptic transmission	6.00	3.00	2.00

Supplementary Table S5D - Differently expressed gene ontology (GO) groups. Biologic processes in negative control versus siDCL-3 comparison. Only GO classes and parent classes with at least 5 observations in the selected subset and with an 'Observed vs. Expected' ratio of at least 2 are shown.

GO id	GO classification	Observed in selected subset	Expected in selected subset	Observed/ Expected
45055	regulated secretory pathway	5.00	0.89	5.61
15986	ATP synthesis coupled proton transport	6.00	1.13	5.32
15985	energy coupled proton transport\, down electrochemical gradient	6.00	1.13	5.32
46916	transition metal ion homeostasis	5.00	0.95	5.26
6119	oxidative phosphorylation	9.00	1.72	5.23
6334	nucleosome assembly	7.00	1.37	5.13
9142	nucleoside triphosphate biosynthetic process	8.00	1.60	4.99
6754	ATP biosynthetic process	6.00	1.25	4.81
6753	nucleoside phosphate metabolic process	6.00	1.25	4.81
9206	purine ribonucleoside triphosphate biosynthetic process	7.00	1.48	4.72
9201	ribonucleoside triphosphate biosynthetic process	7.00	1.48	4.72
9145	purine nucleoside triphosphate biosynthetic process	7.00	1.48	4.72
46034	ATP metabolic process	6.00	1.37	4.39
9205	purine ribonucleoside triphosphate metabolic process	7.00	1.60	4.37
9199	ribonucleoside triphosphate metabolic process	7.00	1.60	4.37
9141	nucleoside triphosphate metabolic process	8.00	1.84	4.35
9144	purine nucleoside triphosphate metabolic process	7.00	1.66	4.21
31497	chromatin assembly	7.00	1.72	4.07
30003	cation homeostasis	6.00	1.48	4.04
6875	metal ion homeostasis	6.00	1.48	4.04
15992	proton transport	6.00	1.54	3.89
7046	ribosome biogenesis and assembly	9.00	2.32	3.89
6873	cell ion homeostasis	6.00	1.60	3.74
9152	purine ribonucleotide biosynthetic process	7.00	1.90	3.68
30005	di-\, tri-valent inorganic cation homeostasis	5.00	1.37	3.66
65004	protein-DNA complex assembly	8.00	2.20	3.64
9260	ribonucleotide biosynthetic process	7.00	2.02	3.47

GO id	GO classification	Observed in selected subset	Expected in selected subset	Observed/ Expected
9108	coenzyme biosynthetic process	9.00	2.61	3.45
50801	ion homeostasis	6.00	1.78	3.37
6818	hydrogen transport	6.00	1.78	3.37
6752	group transfer coenzyme metabolic process	6.00	1.84	3.26
9150	purine ribonucleotide metabolic process	7.00	2.26	3.10
6164	purine nucleotide biosynthetic process	7.00	2.26	3.10
48878	chemical homeostasis	6.00	1.96	3.06
6333	chromatin assembly or disassembly	8.00	2.73	2.93
43039	tRNA aminoacylation	5.00	1.72	2.90
43038	amino acid activation	5.00	1.72	2.90
6418	tRNA aminoacylation for protein translation	5.00	1.72	2.90
9259	ribonucleotide metabolic process	7.00	2.43	2.88
51188	cofactor biosynthetic process	9.00	3.15	2.86
19725	cell homeostasis	6.00	2.14	2.81
6457	protein folding	17.00	6.47	2.63
6163	purine nucleotide metabolic process	7.00	2.73	2.56
6399	tRNA metabolic process	8.00	3.21	2.50
9165	nucleotide biosynthetic process	9.00	3.68	2.44
6118	electron transport	19.00	8.02	2.37
6412	translation	28.00	12.05	2.32
42592	homeostatic process	7.00	3.21	2.18
22613	ribonucleoprotein complex biogenesis and assembly	13.00	6.00	2.17
48534	hemopoietic or lymphoid organ development	5.00	2.32	2.16
30097	hemopoiesis	5.00	2.32	2.16
6732	coenzyme metabolic process	11.00	5.22	2.11
6325	establishment and/or maintenance of chromatin architecture	12.00	5.70	2.11
2520	immune system development	5.00	2.37	2.11

Supplementary Table S5E - Differently expressed gene ontology (GO) groups. Molecular Function in negative control versus siDCL-2 comparison. Only GO classes and parent classes with at least 5 observations in the selected subset and with an 'Observed vs. Expected' ratio of at least 2 are shown.

GO id	GO classification	Observed in selected subset	Expected in selected subset	Observed/ Expected
16676	oxidoreductase activity\, acting on heme group of donors\, oxygen as acceptor	9.00	0.88	10.28
16675	oxidoreductase activity\, acting on heme group of donors	9.00	0.88	10.28
15002	heme-copper terminal oxidase activity	9.00	0.88	10.28
4129	cytochrome-c oxidase activity	9.00	0.88	10.28
50136	NADH dehydrogenase (quinone) activity	13.00	1.75	7.42
8137	NADH dehydrogenase (ubiquinone) activity	13.00	1.75	7.42
3954	NADH dehydrogenase activity	13.00	1.75	7.42
16655	oxidoreductase activity\, acting on NADH or NADPH\, quinone or similar compound as acceptor	13.00	1.94	6.71
15078	hydrogen ion transporter activity	19.00	3.31	5.73
16651	oxidoreductase activity\, acting on NADH or NADPH	13.00	2.38	5.47
15077	monovalent inorganic cation transporter activity	19.00	3.50	5.43
46961	hydrogen ion transporting ATPase activity\, rotational mechanism	7.00	1.31	5.33
46933	hydrogen ion transporting ATP synthase activity\, rotational mechanism	7.00	1.31	5.33
3735	structural constituent of ribosome	34.00	7.75	4.38
19829	cation-transporting ATPase activity	7.00	1.63	4.31
3899	DNA-directed RNA polymerase activity	7.00	1.63	4.31
9055	electron carrier activity	13.00	3.06	4.24
3755	peptidyl-prolyl cis-trans isomerase activity	5.00	1.25	4.00
16859	cis-trans isomerase activity	5.00	1.31	3.81
15405	P-P-bond-hydrolysis-driven transporter activity	10.00	2.94	3.40
15399	primary active transporter activity	10.00	2.94	3.40
51082	unfolded protein binding	14.00	4.50	3.11

GO id	GO classification	Observed in selected subset	Expected in selected subset	Observed/ Expected
42625	ATPase activity\, coupled to transmembrane movement of ions	7.00	2.38	2.95
5198	structural molecule activity	39.00	14.32	2.72
8324	cation transporter activity	24.00	9.51	2.52
16779	nucleotidyltransferase activity	9.00	3.88	2.32
15075	ion transporter activity	25.00	11.82	2.12
3712	transcription cofactor activity	8.00	3.81	2.10

Supplementary Table S5F - Differently expressed gene ontology (GO) groups. Molecular Function in negative control versus siDCL-3 comparison. Only GO classes and parent classes with at least 5 observations in the selected subset and with an 'Observed vs. Expected' ratio of at least 2 are shown.

GO id	GO classification	Observed in selected subset	Expected in Selected subset	Observed/ Expected
16676	oxidoreductase activity\, acting on heme group of donors\, oxygen as acceptor	7.00	0.84	8.37
16675	oxidoreductase activity\, acting on heme group of donors	7.00	0.84	8.37
15002	heme-copper terminal oxidase activity	7.00	0.84	8.37
4129	cytochrome-c oxidase activity	7.00	0.84	8.37
50136	NADH dehydrogenase (quinone) activity	12.00	1.67	7.17
8137	NADH dehydrogenase (ubiquinone) activity	12.00	1.67	7.17
3954	NADH dehydrogenase activity	12.00	1.67	7.17
16655	oxidoreductase activity\, acting on NADH or NADPH\, quinone or similar compound as acceptor	12.00	1.85	6.48
16651	oxidoreductase activity\, acting on NADH or NADPH	12.00	2.27	5.29
15078	hydrogen ion transporter activity	16.00	3.17	5.05
46961	hydrogen ion transporting ATPase activity\, rotational mechanism	6.00	1.25	4.78
46933	hydrogen ion transporting ATP synthase activity\, rotational mechanism	6.00	1.25	4.78
15077	monovalent inorganic cation transporter activity	16.00	3.35	4.78
9055	electron carrier activity	13.00	2.93	4.44
3735	structural constituent of ribosome	29.00	7.41	3.91
19829	cation-transporting ATPase activity	6.00	1.55	3.86
3899	DNA-directed RNA polymerase activity	5.00	1.55	3.22
15405	P-P-bond-hydrolysis-driven transporter activity	9.00	2.81	3.21
15399	primary active transporter activity	9.00	2.81	3.21
51082	unfolded protein binding	13.00	4.30	3.02
3713	transcription coactivator activity	5.00	1.85	2.70
42625	ATPase activity\, coupled to transmembrane movement of ions	6.00	2.27	2.64
3712	transcription cofactor activity	9.00	3.64	2.47

GO id	GO classification	Observed in selected subset	Expected in selected subset	Observed/ Expected
3702	RNA polymerase II transcription factor activity	5.00	2.03	2.46
8324	cation transporter activity	21.00	9.08	2.31
5198	structural molecule activity	31.00	13.68	2.27
16876	ligase activity\, forming aminoacyl-tRNA and related compounds	5.00	2.21	2.26
16875	ligase activity\, forming carbon-oxygen bonds	5.00	2.21	2.26
4812	aminoacyl-tRNA ligase activity	5.00	2.21	2.26
8134	transcription factor binding	9.00	4.06	2.22
16564	transcriptional repressor activity	7.00	3.23	2.17

Supplementary Table S6 - qPCR results of some differently expressed genes. Not signf., not significant; NA, not applied.

	Microarray results		qPCR results		
Gene symbol	**Negative control vs. siDCL-2**	**Negative control vs. siDCL-3**	**Negative control vs. siDCL-2**	**Negative control vs. siDCL-3**	**Validated?**
Mt3	Up-regulated	Up-regulated	Up-regulated	Up-regulated	Yes
Ndufa3	Up-regulated	Up-regulated	Up-regulated	Up-regulated	Yes
Bax	Up-regulated	Up-regulated	Up-regulated	Up-regulated	Yes
Ddx5	Down-regulated	Down-regulated	Down-regulated	Down-regulated	Yes
DCLK-long	Down-regulated	Down-regulated	Down-regulated	Down-regulated	Yes
Bric5	Down-regulated	Down-regulated	Down-regulated	Down-regulated	Yes
DCL	NA	NA	Down-regulated	Down-regulated	NA
Ywhah	Down-regulated	Not signif.	Down-regulated	Not signif.	Yes
Bcl2L13	Down-regulated	Not signif.	Down-regulated	Not signif.	Yes
Tubb3	Down-regulated	Not signif.	Down-regulated	Not signif.	Yes
Plekhh1	Down-regulated	Not signif.	Down-regulated	Not signif.	Yes
Pak2	Not signif.	Down-regulated	Not signif.	Down-regulated	Yes
Ppp2r1a	Not signif.	Down-regulated	Not signif.	Down-regulated	Yes
Zc3hc1	Not signif.	Down-regulated	Not signif.	Down-regulated	Yes
Kif20a	Not signif.	Down-regulated	Not signif.	Down-regulated	Yes